


7-2014

Synthesis and Characterization of Cadmium(II) Complexes with Biologically Inspired Multidentate Ligands

Carolina Rojas Ramirez
College of William and Mary

Follow this and additional works at: <https://scholarworks.wm.edu/honorsthesis>

 Part of the [Biochemistry Commons](#), and the [Inorganic Chemistry Commons](#)

Recommended Citation

Rojas Ramirez, Carolina, "Synthesis and Characterization of Cadmium(II) Complexes with Biologically Inspired Multidentate Ligands" (2014). *Undergraduate Honors Theses*. Paper 112.
<https://scholarworks.wm.edu/honorsthesis/112>

This Honors Thesis is brought to you for free and open access by the Theses, Dissertations, & Master Projects at W&M ScholarWorks. It has been accepted for inclusion in Undergraduate Honors Theses by an authorized administrator of W&M ScholarWorks. For more information, please contact scholarworks@wm.edu.

**Synthesis and Characterization of Cadmium(II) Complexes with Biologically
Inspired Multidentate Ligands**

A thesis submitted in partial fulfillment of the requirement
for the degree of Bachelor of Science with Honors in Chemistry
from the College of William and Mary

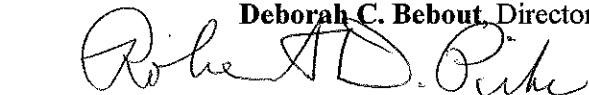
by

Carolina Rojas Ramírez

Accepted for Honors
(Honors, High Honors, Highest Honors)



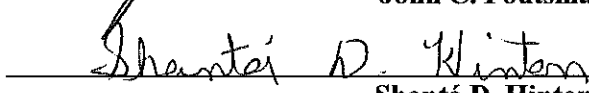
Deborah C. Bebout, Director



Robert D. Pike



John C. Poutsma



Shantá D. Hinton



William R. McNamara

Williamsburg, Virginia
July 29th, 2014

ABSTRACT

The recent discovery of a biologically beneficial role for Cd(II) has motivated further investigation of its coordination chemistry. In this work, multidentate ligands model the geometric constraints associated with protein metal binding environments. The synthesis and characterization of Cd(II) complexes in a 1:1 ratio with 2-[[2-(dimethylamino)ethyl]amino]ethanethiol (**HL**₁), Bis(2-methylpyridyl)diselenide (**L**₂), and tris[(1-methyl-2-imidazolyl)methyl]amine (**L**₃) may contribute to a better understanding of potentially biologically relevant interactions between Cd(II) and imidazoles, thiolates, selenoethers and diselenides.

Three new complexes were synthesized and characterized. Electrospray ionization mass spectrometry of $[(\text{Cd}(\mathbf{L}_1))_6(\mu_3\text{-CO}_3)](\text{ClO}_4)_2$ demonstrated that aromatic nitrogen donors are an optional component of NN'S tridentate ligands forming Cd(II) complexes with CO₂ fixating properties. The new complex $[\text{Cd}(\mathbf{L}_2)(\text{NO}_3)_2]$ was prepared and characterized by X-ray crystallography, confirming that Cd-(SeR)₂ bond formation could be fostered by a chelating ligand. Finally, structural characterization of the new complex $[\text{Cd}(\mathbf{L}_3)(\text{NCCH}_3)](\text{ClO}_4)_2$ revealed a great deal of similarity to the coordination environment of Zn(II) in human carbonic anhydrase B.

TABLE OF CONTENTS

Acknowledgements	ii
List of Tables	iii
List of Figures	iv
List of Ligands	v
List of Compounds Numbers	vi
1. Introduction	1
2. Experimental	12
3. Results and Discussion	20
4. Conclusion	43
References	45

ACKNOWLEDGEMENTS

My participation in this investigation was supported in part by Howard Hughes Medical Institute Science Education Grant to the College of William and Mary. I wish to express my profound gratitude to Professor Deborah C. Bebout, under whose guidance this undertaking was made possible, for her patience, guidance, thoughtfulness, and criticism throughout the investigation. The author is also indebted to Professors Robert D. Pike, John C. Poutsma and Shantá D. Hinton for their careful reading and criticism of the manuscript. Also, thanks Prof. William R. McNamara for being part of my committee.

Special thanks for Prof. Pike for his guidance and help with the crystallographic characterization of the complexes discussed and Prof. Poutsma for providing access to his ESI-MS spectrometer.

Thanks to those students who have contributed directly to this work: Stephanie E. Winslow, Wei Lai, Andrew Tran, William Kaplan, Jonathan Bowman, Benjamin Winer, Malia Hain, and Yoko Fukuda. Thanks finally to my parents and their endless support in order to continue with my education.

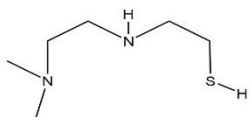
LIST OF TABLES

(1) Crystallographic data for cocrystal of $[\text{Cd}(\mathbf{L}_5)(\text{NO}_3)_2]$ and $[\text{Cd}(\mathbf{L}_2)(\text{NO}_3)_2]$ (6A, 7A), independent crystal of $[\text{Cd}(\mathbf{L}_2)(\text{NO}_3)_2]$ (7B) and $[\text{Cd}(\mathbf{L}_3)(\text{NCCH}_3)](\text{ClO}_4)_2$ (16).	18
(2) Crystallographic data for $[\text{Zn}(\mathbf{L}_7)\text{Cl}_2]$ polymorphs 5A and 5B .	19
(3) Selected bond distances (\AA) and angles ($^\circ$) in $[\text{Zn}(\mathbf{L}_7)\text{Cl}_2]$ polymorphs 5A and 5B .	29
(4) Selected bond distances (\AA) in 6, 7A and 7B .	34
(5) Selected angles ($^\circ$) in 6, 7A and 7B .	35
(6) Overview of structurally characterized mononuclear complexes with M- (Se_2R_2) bonds.	38
(7) Selected bond distances (\AA) and angles ($^\circ$) in (16).	41

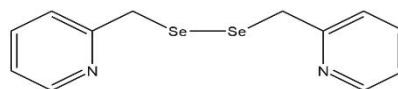
LIST OF FIGURES

(1)	Multidentate ligands used in this study.	2
(2)	N,N,S tridentate ligands.	8
(3)	Space-filling diagrams of the 1^{2+} and 3^{2+} cations.	9
(4)	Bicyclic $[\text{Cu}(\text{L}_2)\text{X}_2]$ and macrocyclics $[\text{Co}(\text{L}_2)\text{X}_2]$ and $[\text{Zn}(\text{L}_2)\text{X}_2]$.	11
(5)	Synthesis of HL₁ .	13
(6)	Synthesis of HL₂ .	14
(7)	$^1\text{HNMR}$ spectra in CD_3NO_2 of HL₁ , 14 and 15 .	22
(8)	FITR Spectra for HL₁ , 14 and 15 .	23
(9)	ESI-MS spectra for CH_3CN solutions of 14 and 15 .	25
(10)	Calculated and observed isotope patterns for $[(\text{CdL}_1)_6(\text{CO}_3)_2]^{2+}$.	26
(11)	ORTEP diagram of $[\text{ZnL}_7\text{Cl}_2]$ polymorphs 5A and 5B .	27
(12)	Structural overlay of 5A and 5B .	28
(13)	Packing diagram for 5A .	30
(14)	Packing diagram for 5B .	30
(15)	$^1\text{HNMR}$ spectra of 6 and 7B .	32
(16)	ORTEP diagram of $[\text{Cd}(\text{L}_2)(\text{NO}_3)_2]$ (7B).	33
(17)	Structural overlay of 7A and 7B .	36
(18)	Packing diagram for 7A and 7B .	37
(19)	ORTEP diagram of $[\text{CdL}_3(\text{NCCH}_3)](\text{ClO}_4)_2$ (16).	40
(20)	Packing diagram for 16 .	40
(21)	$^1\text{HNMR}$ spectra of 16 .	42

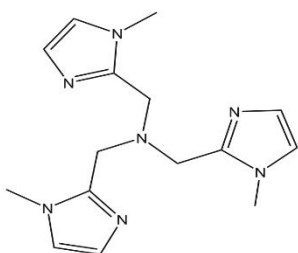
LIST OF LIGANDS



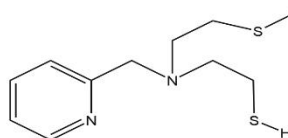
2-[[2-(dimethylamino)ethyl]amino]ethanethiol
(HL₁)



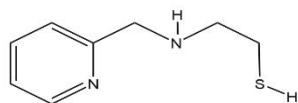
bis(2-methylpyridyl)diselenide
(L₂)



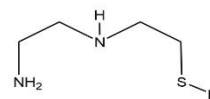
tris[(1-methyl-2-imidazolyl)methyl]amine
(L₃)



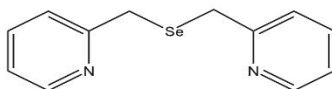
2-[[2-(methylthio)ethyl](2-pyridylmethyl)amino]ethanethiol
(HL₄)



2-[(2-pyridylmethyl)amino]ethanethiol
(HL₅)



2-[(2-aminoethyl)amino]ethanethiol
(HL₆)



bis(2-methylpyridyl)selenide
(L₇)

LIST OF COMPOUNDS NUMBERS

- (1) $[(\text{Cd}(\mathbf{L}_4))_6(\mu_3\text{-CO}_3)_2](\text{ClO}_4)_2$
- (2) “ $\text{Cd}(\mathbf{L}_4)(\text{ClO}_4)$ ”
- (3) $[(\text{Cd}(\mathbf{L}_5))_6(\mu_3\text{-CO}_3)_2](\text{ClO}_4)_2$
- (4) “ $\text{Cd}(\mathbf{L}_5)(\text{ClO}_4)$ ”
- (5) $[\text{Zn}(\mathbf{L}_7)\text{Cl}_2]$
- (6) $[\text{Cd}(\mathbf{L}_7)(\text{NO}_3)_2]$
- (7) $[\text{Cd}(\mathbf{L}_2)(\text{NO}_3)_2]$
- (8) $[\text{Cu}(\mathbf{L}_2)\text{X}_2]$
- (9) $[\text{Co}(\mathbf{L}_2)\text{X}_2]$
- (10) $[\text{Zn}(\mathbf{L}_2)\text{X}_2]$
- (11) $[\text{Hg}(\mathbf{L}_3)_2](\text{ClO}_4)_2$
- (12) $[\text{Hg}(\mathbf{L}_3)(\text{NCCH}_3)](\text{ClO}_4)_2$
- (13) $[\text{Hg}(\mathbf{L}_3)\text{Cl}]_2(\text{HgCl}_4)$
- (14) $[(\text{Cd}(\mathbf{L}_1))_6(\mu_3\text{-CO}_3)_2](\text{ClO}_4)_2$
- (15) “ $\text{Cd}(\mathbf{L}_1)(\text{ClO}_4)$ ”
- (16) $[\text{Cd}(\mathbf{L}_3)(\text{NCCH}_3)](\text{ClO}_4)_2$

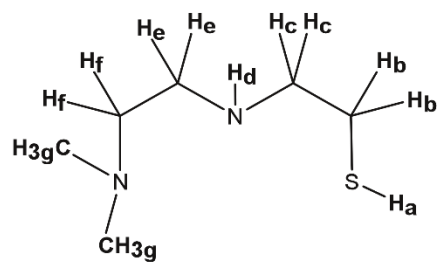
Synthesis and Characterization of Cadmium(II) Complexes with Biologically Inspired Multidentate Ligands

1. Introduction

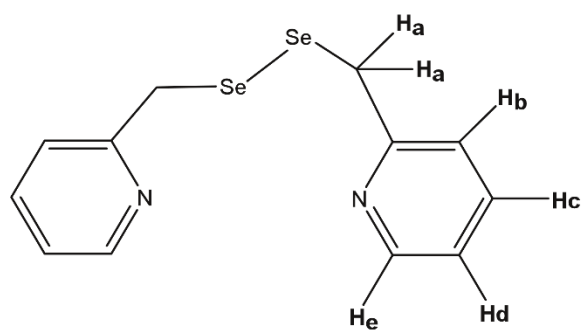
Proteins are the cellular workers that sustain life. These complex and unique macromolecules are able to participate in a wide range of processes such as signal transduction, metabolism, immunity, and cellular differentiation, just to name a few. This diversity of function sometimes requires incorporation of a cofactor, such as metal ions. At catalytic centers, metals increase acidity, electrophilicity and/or nucleophilicity of reacting species, promote heterolysis, or receive and donate electrons.¹ It is important to appreciate the role protein structure has in determining the function of a metalloprotein. The protein's primary and secondary metal coordination spheres adjust the properties of the metal to enhance reactivity and influence metal selection, while donor ligands (for example S, O or N) can favor binding to the correct metal.²

Crystallographic and countless mutation studies have demonstrated that the elimination or replacement of active site residues can greatly diminish or completely eliminate metalloprotein function by negatively affecting metal-binding. In order to accurately model metalloprotein active site models, it is important to design and synthesize metal chelates capable of stabilizing both primary and secondary coordination environments.³

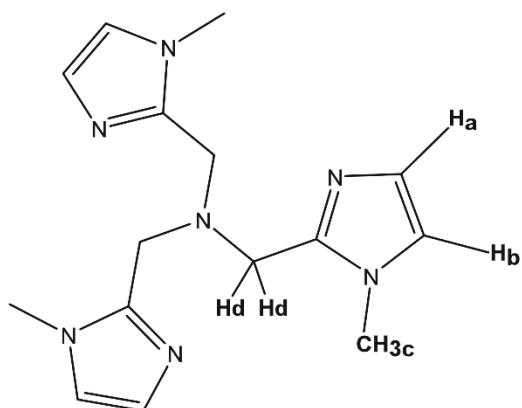
Multidentate ligands model the geometric constraints associated with protein metal binding environments and have proven useful for the preparation of functional mononuclear complexes for further analysis.³ The focus of this study is biologically relevant cadmium(II) multidentate ligand interactions (Fig. 1). Related coordination chemistry of Zn(II) is also explored.



2-[[2-(dimethylamino)ethyl]amino]ethanethiol (**HL₁**)



bis(2-methylpyridyl)diselenide (**L₂**)



tris[(1-methyl-2-imidazolyl)methyl]amine (**L₃**)

Figure 1. Multidentate ligands used in this study.

In a metal complex the metal ion acts as a Lewis acid, while the ligand acts as a Lewis base. At the same time, the metal and ligand can be classified according to their hardness or softness. In this context, soft indicates large, polarizable atoms with easily distorted clouds of electrons, while hard implies small, nonpolarizable atoms. Hard-hard and soft-soft metal-ligand interactions are generally stronger than their hard-soft counterparts. In the Zn triad, Zn is the hardest of the group, Cd is medium, and Hg is soft. The elusiveness of the Zn-Se bond is partially due to the relative weakness of interactions between hard Zn with soft Se. In this work, multidentate chelating ligands providing an entropic enhancement for M-SeR₂ and M-(Se₂R₂) interactions with marginal enthalpic favorability are investigated.

Multidentate ligands also provide a convenient manner of limiting solution speciation for d¹⁰ metal ions such as Zn(II).⁴ In addition, as synthetic models of protein metal binding sites they can reveal differences between the coordination behavior of physiologically essential metal ions and their more toxic congeners. For example, cadmium(II) is known for its extreme toxicity to mammals, which is thought to be caused in part by its ability to substitute for Zn(II) in enzymes. Interestingly, ¹¹³Cd has often been employed as a metalloprobe, and in the last decade the first beneficial biological function for this highly toxic metal was discovered.^{5,6}

1.1 Cadmium coordination chemistry with biologically-relevant chalcogen-containing multidentate ligands

The term “chalcogen” was proposed around 1930 by Werner Fischer to denote the elements of Group 16.⁷ On account of their *ns²np⁴* outer electronic configurations, the chemistry of the lighter chalcogens is non-metallic.⁷ Tellurium is a metalloid and polonium is a highly radioactive metal. Neither tellurium nor polonium have biological functions, unlike oxygen, sulfur, and the micronutrient selenium.

The identified physiological roles of the chalcogens are diverse. Oxygen is essential for redox chemistry, aerobic respiration, immunity, where macrophages employ Reactive Oxygen Species to eliminate bacteria, and much more. Sulfur is known for its roles in stabilization of tertiary protein structure through disulfide bonds, involvement in fat metabolism and detoxification process, and many others. The essentiality of selenium to mammals was recognized in the 1950's and since then selenoproteins with roles in thyroid hormone production, intracellular redox status equilibrium, antioxidation, prooxidation and more have been identified.⁸ L-selenomethionine (SeMet) has a high bioavailability and low toxicity and is therefore a popular form for dietary supplementation.⁸ Dietary SeMet is either metabolized or stored in proteins by tRNAMet, which does not discriminate between SeMet and methionine.⁴ The transsulfuration pathway that is responsible for the synthesis of cysteine (Cys) from Met also transforms SeMet into SeCys.⁸ Analogous to the adventitious incorporation of SeMet into proteins in place of Met, SeCys can be incorporated in place of Cys and released upon degradation of these proteins and selenoproteins.⁸ Protein structure is usually unaffected by the misincorporation of the selenoamino acids.^{4,8} Nonetheless, substitution near the active site can alter enzyme activity due to the chemical differences between selenium and sulfur. The greater atomic radius of selenium compared to sulfur results in weaker bonding to carbon and hydrogen in selenium compounds than in their sulfur analogues.⁴

The synthesis and characterization of two novel cadmium(II) complexes with chalcogenic multidentate ligands will be explored. The goal of these studies is to prepare and characterize complexes providing new insight regarding the potentially biologically relevant interactions of Cd(II) with thiolates, selenoethers and diselenides. Answers to questions such as “what does global warming has to do with a Cd(II) macrocycle?” will be revealed.

1.1.1 Cadmium Carbonic Anhydrase Inspired Coordination Chemistry

The rising atmospheric level of carbon dioxide (CO₂), an greenhouse gas, is the single most important factor contributing to anthropogenic climate change and warming sea surface temperatures.⁹ Anthropogenic CO₂ emissions will likely continue to increase over the next several decades unless there are dramatic changes in carbon and energy policy.¹⁰ The greatest effects of CO₂ accumulation in the atmosphere are extreme weather events and ocean acidification, which will result in extinction of species if unchecked. The ocean is a critical component of Earth's climate system, acting to slow climate change by storing excess heat and by removing excess CO₂ from the atmosphere.⁹ The protagonists for overcoming the difficulties of CO₂-fixation in the ocean are photosynthetic organisms.

The limited capacity of water to retained CO₂(gas), as well as the 10⁻⁴ times slower diffusion rate of CO₂(aq) in water than in the atmosphere, makes the ocean a CO₂-poor environment.¹¹ To maintain efficient photosynthesis in spite of low CO₂ availability, many phytoplankton species possess a carbon-concentrating mechanism (CCM) generally thought to have two key components: a mechanism for directly or indirectly taking up bicarbonate (HCO₃⁻, the predominant form of dissolved inorganic carbon in marine environments) and carbonic anhydrase (CA).¹²

Among the fastest enzymes known, with turnover numbers close to one million per second, carbonic anhydrases catalyze the dehydration of HCO₃⁻ to CO₂ required in the first step of the Calvin cycle.¹³ This ubiquitous metalloenzyme has five forms across taxonomic kingdoms with no significant sequence or structural homology.¹⁴ The α and β forms are Zn(II)-dependent CAs, however γ -CAs are cambialistic enzymes – able to use either Zn(II), Fe(II) and Co(II) ions for catalysis.¹³ Whereas α - and γ -CA use three histidine residues to coordinate the Zn atom, β -CA uses two cysteine residues and one histidine residue.¹⁵

Diatoms, which are one of the most common types of phytoplankton and are widespread in oceans, possess CAs fundamental for acquisition of inorganic carbon.¹¹ The δ and ζ forms were

discovered in the model species *Thalassiosira weissflogii*. The first member of the δ -CAs was *Thalassiosira weissflogii* Carbonic Anhydrase 1 (TWCA1), a 27 kDa protein with a similar active site to that of the better characterized α -CAs, but no sequence homology.¹⁶ The catalytic zinc ion is coordinated by three histidine ligands and a single water molecule.¹¹ In the marine environment, phytoplankton have to adapt to the low concentration of CO₂ as well as very low concentrations of physiologically essential metal ions such as Zn(II) in surface seawater.⁶ Further studies revealed upregulation of TWCA1 by low pCO₂ and *in vivo* replacement of Zn(II) by Co(II) under Zn-limited conditions.¹¹ A second novel cambialistic carbonic anhydrase was produced by this marine diatom under Zn(II)-limited conditions with the surprising twist of Cd(II) in its active site. Dubbed CDCA1, this enzyme established the ζ -CA class. It was found to revert to a Zn(II) enzyme with slightly higher activity.¹⁵

Cadmium Carbonic Anhydrase 1 (CDCA1), is a novel 69 kDa enzyme consisting of three repeats (R1, R2 and R3) sharing 85% identity in their primary sequences.¹⁵ Xu *et al.* performed structural analysis of R1 and R2 in four distinct forms: cadmium-bound, zinc-bound, metal-free and acetate bound, revealing a novel fold for these domains.¹⁵ In the active site, Cd(II) is coordinated by three invariant residues in CDCA of all diatom species: Cys 263, His 315 and Cys 325.¹⁵ The distances between Cd(II) and the metal-binding atoms of these residues (S γ of Cys 263, N ϵ_2 of His 315 and S γ of Cys 325) are 2.46 Å, 2.34 Å and 2.51 Å, respectively.¹⁵ Additional species bound to Cd(II) include a water oxygen completing tetrahedral coordination at 2.35 Å and a second water oxygen bound at a distance of 2.65 Å.¹⁵ Additional highly conserved residues at the active site of CDCA1 include Asp 265 and Arg 267. The C α atoms of the five highly conserved active site residues can be superimposed with those of β -CA from *Pisum sativum* with an r.m.s. deviation of 0.73 Å.¹⁵ The locations of the catalytic metal ion and its tetrahedrally bound water molecule are also nearly identical between CDCA1 and β -CA. CDCA1 is inactivated by mutation of any of these five conserved residues.¹⁵ The structural analysis performed by Xu *et al.* also provided a plausible

explanation for the spontaneous exchange of Zn(II) and Cd(II) in the active site of CDCA1: “A conserved sequence between two metal-coordinating residues adopts a stable open conformation in the metal-free protein which effectively lowers the free energy penalty of releasing the bound metal and hence facilitates metal exchange.”¹⁵

Recently, Alterio *et al.* completed the X-ray characterization of CDCA-R3 and built a docking model of the full length enzyme.¹¹ The CDCA-R3 structure consists of seven α -helices, three 3_{10} -helices and three β -sheets, as observed already for the other repeats.¹¹ In the active site a slightly distorted trigonal-bipyramidal geometry of Cd(II) is generated by metal ion coordination with Cys473, His525, Cys535, a water molecule and an acetate ion (derived from the crystallization solution), as previously observed for the acetate bound forms of CDCA1-R1 and CDCA1-R2.¹¹

As increasing atmospheric CO₂ contributes to global environmental problems, the development of novel techniques that decrease this greenhouse gas is of great significance. CDCA active site structure might hold the key to developing those techniques.

1.1.1.1 Previous studies of CO₂ fixation with Cd(II) complexes

In many Zn enzymes the functional metal ion is surrounded by a N_XS_Y donor set provided by the amino acids histidine and cysteine, respectively.¹⁷ Tridentate N,N,S ligands have been found to form metal compounds that can mimic metal-sulfur coordination in biological systems due to the great variability of their coordinative behavior toward the metal ion.¹⁷⁻²²

Recently, an novel bis-carbonate macrocyclic complex [(Cd(L₄))₆(μ_3 -CO₃)₂] (ClO₄)₂ (**1**) was formed in air-exposed solutions of the tridentate N,N,S ligand 2-[[2-(methylthio)ethyl](2-pyridylmethyl)amino]ethanethiol (**HL**₄), Cd(ClO₄)₂ and triethylamine (NEt₃) in wet acetone.²³ Although air contains less than 0.04 mole percent CO₂, self-assembly of **1** occurred with fixation of two CO₂ molecules from air. The self-assembly properties of this new complex were confirmed by preparing the air-free precipitate “Cd(L₄)(ClO₄)” (**2**), which was converted to **1** within minutes

of introducing base and CO₂, providing the first documentation of rapid CO₂ fixation by a Cd(II) complex.²³ Interestingly, saturated alkylthiolate ligands bind the Cd(II) in **1** and the ζ-CAs, as well as Zn(II) in the β-CAs, and they all share carbon fixation properties.²³

Later, the synthesis and characterization of the complex [(Cd(L₅))₆(μ₃-CO₃)₂](ClO₄)₂ (**3**) demonstrated that ligands without the pendant thioether group of **HL**₄ would retain (CdS)₆(μ₃-CO₃)₂ core-forming abilities (Fig. 2).²⁴ Complex **3** was crystallized from an acetone solution containing 2-[(2-pyridylmethyl)amino]ethanethiol **HL**₅, Cd(ClO₄)₂ and NEt₃ exposed to a CO₂ enriched environment.²⁴ As previously done with **1** and **2**, “CdL₅ClO₄” (**4**) was prepared air-free and its rapid transformation to **3** following treatment with base and CO₂ was confirmed by both ¹H NMR and ESI-MS.²⁴ Could there be other features in N,N,S tridentate ligands, besides the pendant thioether group from **HL**₄, that are nonessential to formation of a (CdS)₆(μ₃-CO₃)₂ core? The sterically demanding pyridyl rings in **HL**₄ and **HL**₅ seem to provide stabilizing π-π stacking interactions and to limit carbonate solvent exposure (Fig. 3).²⁴ In this study 2-[(2-aminoethyl)amino]ethanethiol (**HL**₆) and 2-[[2-(dimethylamino)ethyl]amino]ethanethiol (**HL**₁) will be explored for Cd(II) coordination and carbon fixation studies (Fig. 2).

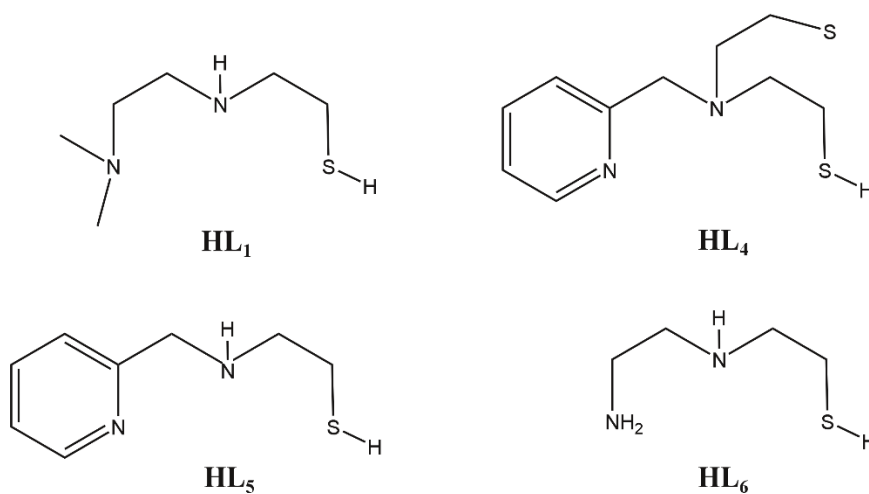


Figure 2. Ligands with a NN/S donor group used in CO₂-fixating studies.

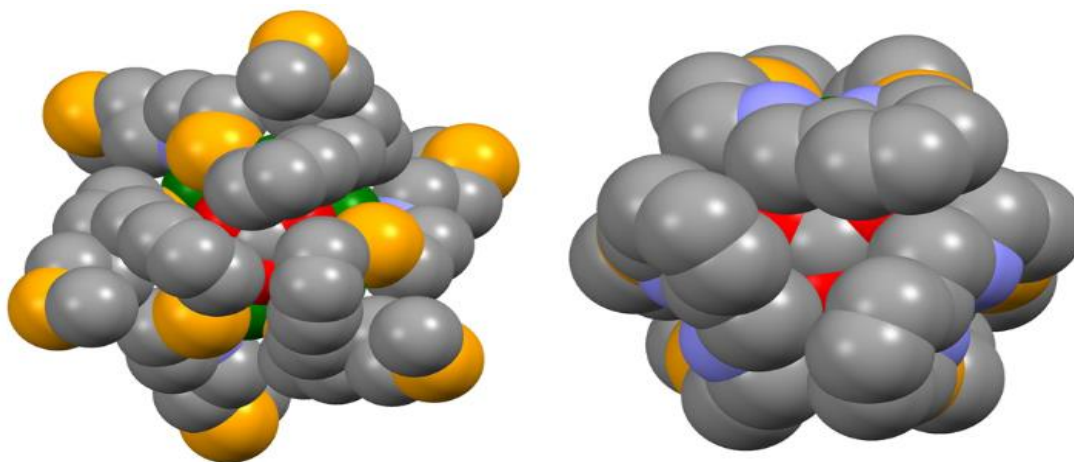


Figure 3. Space-filling diagram of the 1^{2+} (left) and 3^{2+} (right) cations looking down the C_3 axis.

To date, no metal complexes containing both carbonate and either L_6 or L_1 have been reported. The structurally characterized complexes of L_6 include $[ZnL_6]_n(ClO_4)_{2n}$,¹⁹ $[Zn\{Zn(L_6)_2\}_2](ClO_4)_2 \cdot CH_3CN$,¹⁹ $[Pd_4L_6]Cl \cdot CH_3OH \cdot H_2O$,²⁰ $[Fe\{Fe(L_6)_2\}_2](ClO_4)_2 \cdot CH_3OH$,²¹ and $[MnL_6Cl_n]$.²² Mikuriya *et al.* prepared 1:1 complexes of $Cd(ClO_4)_2$ with L_6 by precipitation, but only infrared spectroscopy was used for characterization and the possibility of carbonate coordination was not explored.¹⁸ The structurally characterized complexes of L_1 include $(MoL_1O_2)_2(\mu-O)$,²⁵ and $(MoL_1O_2)(MoL_1O(diphenylhydrazido))(\mu-O)$.²⁶

1.1.2 Investigating interactions between divalent Group 12 metal ions and neutral selenides with mixed N,Se ligands

Selenium is known to protect against $Hg(II)$ and $Cd(II)$ toxicity, however the mechanism is not well understood.²⁷ Gasiewicz *et al.* were able to partly recover cadmium and selenium in equimolar high molecular-weight (HMW) protein complexes when simultaneously administered to rats.²⁸ In order to obtain these complexes in rat plasma, the prior conversion of selenite to selenide is required. Interestingly, Hg interacts with Se in a similar manner.^{29,30} Until recently, the only Group 12 metal

ion with crystallographically documented binding to neutral selenide ligands was Hg(II). Studies conducted by Winer *et al.* explored the coordination chemistry of all the divalent Group 12 metal ions with the tridentate ligand bis(2-methylpyridyl)selenide (**L**₇).⁴ Using perchlorate salts and a 1:2 metal:ligand ratio, the first metal complex with a Cd-SeR₂ bond was structurally characterized, as well as the highest coordination number complex with a Hg-SeR₂ bond yet to be reported. However, a comparable Zn(II) complex proved elusive.⁴

Additional studies of divalent Group 12 metal ions with **L**₇ were conducted with chloride salts and a 1:1 metal:ligand ratio. In addition to preparing [(Cd**L**₇Cl)₂(μ-Cl)₂], a second complex with Cd-SeR₂ bonding, Winslow *et al.* identified two macrocyclic polymorphs of the complex [Zn(**L**₇)Cl₂] (**5**).²⁷ The complex was asymmetric in the major polymorph (**5A**) and had a C₂ axis in the minor polymorph (**5B**). As part of this work, the crystal structure of **5A** was resolved at 150 K to allow for more direct comparison to the structure of **5B**.

Continued interest in crystallographically documenting Zn-SeR₂ bonding interactions led to investigation of the coordination chemistry of **L**₇ with the nitrate salts of the divalent Group 12 metal ions. These efforts produced bicyclic [Zn**L**₇(NO₃)₂], the first structurally characterized complex with a bonding Zn-SeR₂ interaction. For comparison, bicyclic [Cd(**L**₇)(NO₃)₂] (**6**) was structurally characterized.²⁷ This complex was initially synthesized in a relatively modest volume of acetonitrile and crystallized from the supernatant. As a result, trace ligand contamination with bis(2-methylpyridyl)diselenide (**L**₂) was inadvertently exacerbated and **6** was cocrystallized with 15% bicyclic [Cd(**L**₂)(NO₃)₂] (**7A**). In this work, **L**₂ is synthesized and [Cd(**L**₂)(NO₃)₂] (**7B**) is prepared as an independent species for structural comparison. Based on a search of the Cambridge Crystallographic Database (v. 5.32 updated Nov 2013), the only known complexes of **L**₂ are bicyclic [Cu(**L**₂)X₂]³² (**8**) and macrocyclic [Co(**L**₂)X₂]³² (**9**) and [Zn(**L**₂)X₂]³² (**10**) (Fig. 4).

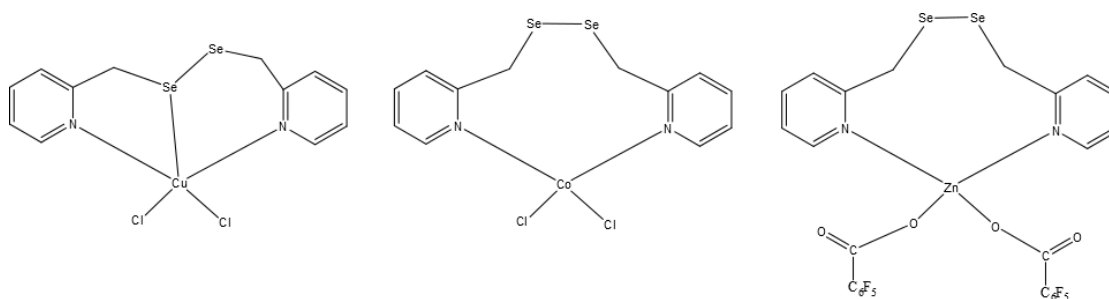


Figure. 4 Bicyclic $[\text{Cu}(\text{L}_2)\text{X}_2]$ (**8**) and macrocyclic $[\text{Co}(\text{L}_2)\text{X}_2]$ (**9**) and $[\text{Zn}(\text{L}_2)\text{X}_2]$ (**10**).

1.2 α/δ -Carbonic Anhydrase modeling with multidentate imidazolyl ligands

To complement our studies related to the active sites of the β -CA and ζ -CA classes, the tridentate ligand tris[(1-methyl-2-imidazolyl)methyl]amine (L_3) was used as a model of the active site of α -CA and δ -CA and its Cd(II) coordination chemistry was investigated. L_3 has previously been used as an analog of the imidazole functionality of histidine.^{3,33-35} Bebout *et al.* investigated the coordination chemistry of Hg(II) with L_3 in order to explore the potential of ^{199}Hg NMR as a metalloprobe of proteins.³⁵ The three structures reported previously, $[\text{Hg}(\text{L}_3)_2](\text{ClO}_4)_2$ (**11**), $[\text{Hg}(\text{L}_3)(\text{NCCH}_3)](\text{ClO}_4)_2$ (**12**) and $[\text{Hg}(\text{L}_3)\text{Cl}]_2(\text{HgCl}_4)$ (**13**), highlighted the differences in donor capacity of imidazolyl and aliphatic amine ligands as well as the demanding sterics of five-membered chelate rings involving imidazolyl donors.³⁵ Additional studies of L_3 with physiologically essential metal ions would complement the existing literature. A wide variety of Zn(II) proteins have been substituted with Cd(II) and investigated by ^{113}Cd NMR spectroscopy to gain valuable insight.⁵ Roziere *et al.* performed ^{113}Cd NMR Studies of $^{113}\text{Cd}(\text{II})$ -substituted human carbonic anhydrase B (HCAB).³⁶ NMR spectra were taken of the $^{113}\text{Cd}(\text{II})$ -substituted HCAB with addition of one and two equivalents of K^{13}CN . A resonance centered at 410 ppm with line width ~ 50 Hz was split into a doublet with $J_{\text{CdC}} = 1,060$ Hz, the largest measured ^{113}Cd - ^{13}C coupling constant at the time.³⁶ This indicates binding to one equivalent of CN^- with a Cd-C bond lifetime

of $>10^{-2}$ s.³⁶ In the current study, the coordination chemistry of Cd(II) with **L**₃ in a 1:1 ratio will be explored.

2. Experimental

2.1. Reagents and Methods

Solvents and reagents were of commercial grade and used as received unless otherwise noted. ¹H NMR spectra were recorded in 5-mm-o.d. NMR tubes on a Varian Mercury 400VX or Agilent DD2 operating in the pulse Fourier transform mode. Chemical shifts (in ppm) were measured relative to solvent (δ CDCl₃ 7.27 ppm; CD₃NO₂ 4.33 ppm; CD₃CN 1.94 ppm). Coupling constants are reported in Hz. Reported concentrations of NMR samples are nominal. X-ray crystallography data collection was carried out using graphite-monochromated Cu K α radiation ($\lambda = 1.5418 \text{ \AA}$) on a Bruker SMART Apex II diffractometer with CCD detector. Elemental analyses were performed by Atlantic Microlabs, Inc. of Norcross, GA.

2.2. Syntheses

2.2.1. 2-[[2-(dimethylamino)ethyl]amino]ethanethiol (**HL**₁)

This synthesis is a combination of two established procedures (Fig. 5).^{37,38} All steps are carried out under argon except the vacuum filtration. Dry toluene was prepared by distillation from CaH₂. A solution of N,N-dimethylethylenediamine (10 mL, 95 mmol) in 50 mL dry toluene was heated to reflux under argon with stirring. A solution of excess ethylenesulfide (10 mL, 189 mmol) in 38 mL dry toluene was added dropwise. Refluxing and stirring continued for 3.33 hr with considerable formation of a white polymeric material.

The cooled reaction mixture was vacuum filtrated through celite to remove the polymer. Most of the toluene was removed by distillation at atmospheric pressure. Vacuum distillation (57 °C, 2 – 3 mmHg) provided **HL**₁ as a colorless liquid (3.20 g, 23 %) with adequate purity for additional studies; ¹H NMR (CDCl₃): δ 2.959 (t, ³J_{HH} = 6.55 Hz, unidentified impurity), 2.834 (t, 2H, ³J_{HH} = 6.55 Hz, H_c), 2.711 (q, 4H, ³J_{HH} = 6.16 Hz, H_{b,e}), 2.680 (q, 4H, ³J_{HH} = 6.16 Hz, H_{b,e}), 2.430 (t, 2H, ³J_{HH} = 6.15 Hz, H_f), 2.241 (s, 6H, H_g), 1.751 (s, 2H, H_{a,d}).

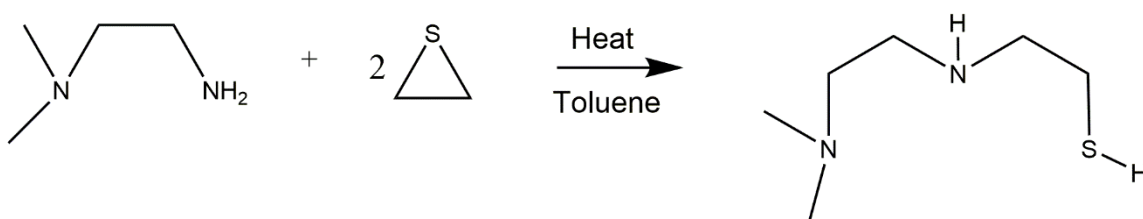


Figure 5. Synthesis of **HL**₁.

2.2.2. Bis(2-methylpyridyl)diselenide (**L**₂)

Bis(2-methylpyridyl)diselenide was prepared by the procedure of Bhasin *et al.* (Fig. 6)³⁹ A solution of diisopropylamine (2.25 mL, 16 mmol) and dry THF (10 mL) in an oven-dried, argon-flushed three-neck roundbottom flask fitted with a stirring bar and thermometer was cooled to -28 °C in a dry ice bath. Lithiumdiisopropylamine (LDA) was prepared by dropwise addition of 1.6 M n-BuLi in hexanes (10 mL, 16 mmol) while maintaining the temperature below -20 °C. The light yellow solution was placed in an ice bath and stirred for 30 min. to complete formation of LDA. After cooling the solution to -78 °C in an acetone/dry ice bath, freshly distilled 2-picoline (1.6 mL, 16 mmol) was added dropwise over 20 min. As the addition progressed, the solution became redder and eventually turned neon orange. The solution solidified while stirring at -78 °C for 30 min. Elemental selenium (1.26 g, 16 mmol) was added. As the reaction mixture was slowly brought to room temperature to dissolve all the selenium it developed a dark-bloody-red color. This solution

the very pale yellow solution for 30 minutes, resulting in the formation of a white precipitate. The solid was collected by vacuum filtration and dried *in vacuo* (99.4 mg, 50.2%). The supernatant was divided into five 2 mL aliquots that were set aside for slow evaporation. MP: 212 °C (dec). Found: C, 25.34 ; H, 4.82 ; N, 8.70 . $C_{38}H_{90}Cd_6Cl_2N_{12}O_{14}S_6$ (for $[(Cd(L_1))_6(\mu_3-CO_3)](ClO_4)_2$ with less than 5% $HNEt_3ClO_4$ requires C, 24.33 ; H, 4.83; N, 8.96 %) 1H NMR (CD_3NO_2 , 7.4 mg/mL, 20 °C): δ 3.058 – 2.902 (m), 2.861 – 2.218 (m), 2.097 (s), 1.330 (s) FTIR (KBr, cm^{-1}) 752, 1085, 1161, 1269, 1370, 1454, 1557, 1649, 1700, 1733, 2338, 2360.

2.2.4. Air free preparation of “ CdL_1ClO_4 ” (15)²³

Solid $Cd(ClO_4)_2 \cdot 6H_2O$ (239 mg, 0.57 mmol) and a solution of **HL**₁ (84 mg, 0.57 mmol) with freshly distilled Et_3N (60 μ L, excess) in 7 mL of 1:1 H_2O :EtOH were placed on opposite sides of a Schlenk-style glass frit. The solution was degassed using two freeze/evacuate/thaw/Ar flush cycles. The solution was added to the metal and stirred under argon for 4 hrs of stirring. No precipitate formed. The solvent was removed *in vacuo*. A residue composed of both a white solid and a clear yellow viscous oil was obtained (0.5978 g). After 3 days in a closed vial, the recovered oil turned dark purple. As time progressed, the amount of solid present decreased and the purple color became lighter. FTIR (KBr, cm^{-1}): 628, 1088, 1110, 1142, 1465. 1H NMR after color change (CD_3NO_2 , 1.7mg/mL): δ 3.415 – 3.339 (m), 3.147 (s), 2.645 (br d, J_{HH} : 8.4 Hz), 2.139 (s), 1.375 (t, J_{HH} = 7.15 Hz).

2.2.5. $[Cd(L_2)(NO_3)_2]$ (7B)²⁷

A solution of $Cd(NO_3)_2 \cdot 4H_2O$ (31.2 mg, 101 μ mol) in 5 mL CH_3CN was added to a solution of **L**₂ (34 mg, 99 μ mol) in 5 mL CH_3CN with stirring. During the addition, the initially clear yellow solution slowly turned reddish-pink. A light rose-brown precipitate formed while stirring the solution for 1 hr. The solid residue was collected using a fine grade sintered glass vacuum funnel (30 mg, 58%). MP: 121°C (dec) (Found: C, 24.86 ; H, 2.08; N, 9.56. $C_{12}H_{12}CdN_4O_6Se$ requires C,

24.91; H, 2.09 ; N, 9.68 %); ^1H NMR (CD_3CN , 3 mM): δ 8.6372 (m, 2H, H_c), 7.984 (m, 2H, $^3J_{\text{HH}} = 7.8$ Hz, $^4J_{\text{HH}} = 1.7$ Hz, H_c), 7.543 (d, 2H, $^3J_{\text{HH}} = 7.8$ Hz, H_b), 7.54 – 7.50 (m, 2H, H_d), 4.216 (s, 4H, $J_{\text{SeH}} = 17.8$ Hz, H_a).

To prepare X-ray quality crystals of a solution of $\text{Cd}(\text{NO}_3)_2 \cdot 4\text{H}_2\text{O}$ (25 mg, 81 μmol) in 5 mL CH_3CN was added to a solution of **L**₂ (28 mg, 82 μmol) in 5 mL CH_3CN with stirring. After 15 minutes, the initially pale yellow solution developed a red tint and slight cloudiness. The solution was filtrated through celite to remove the red material. The clear yellow filtrate was divided into five 2 mL aliquots that were set aside for slow evaporation. X-ray quality crystal were obtained after two weeks. A crystal measuring 0.40 x 0.20 x 0.16 mm was glued on the end of a glass fiber. The data were collected using the θ – 2θ technique over a θ range of 3.243 to 66.993°. The final data to parameter ratio was 12.88:1. Crystallographic data for **7B** and its polymorph **7A** isolated as part of a cocrystal with **6A** are provided in Table 1.

2.2.6. $[\text{Cd}(\text{L}_3)(\text{NCCH}_3)](\text{ClO}_4)_2$ (**16**)

Previously prepared **L**₃ was used to prepare **16**.³⁵ A solution of $\text{Cd}(\text{ClO}_4)_2 \cdot 6\text{H}_2\text{O}$ (67 mg, 0.16 mmol) in 3.5 mL CH_3CN was added to a solution of **L**₃ (48 mg, 0.16 mmol) in 2 mL CH_3CN with stirring. Toluene (2.5 mL) was added slowly to the pale yellow solution with stirring. The solution was filtered through celite. Filtrate aliquots (2 mL) were brought close to saturation with toluene (2.5 mL) and set aside for slow evaporation. Colorless X-ray quality crystals formed upon standing in less than 24 hrs. Following removal of the mother liquor, crystals became white over a period of hours. Based on elemental analysis, acetonitrile was replaced by water. A crystal mounted promptly after mother liquor removal was sufficiently stable at 100 K for diffraction analysis. Yield: 31 mg (30%); mp (after $\text{CH}_3\text{CN}/\text{H}_2\text{O}$ exchange) 173 °C (dec.) Found: C, 27.91 ; H, 3.66 ; N, 15.05 . $\text{C}_{15}\text{H}_{23}\text{CdCl}_2\text{N}_7\text{O}_9$ (for $[\text{Cd}(\text{L}_3)(\text{OH}_2)](\text{ClO}_4)_2$) requires C, 28.66 ; H, 3.69; N, 15.59 %); ^1H NMR (CD_3CN , 10 mM): δ 7.130 (ddd, 1H, $^3J_{\text{HH}} = 1.5$ Hz, $J_{\text{CdH}} = 4.9$ Hz, H_b), 7.092 (ddd, 1H, $^3J_{\text{HH}} = 1.5$

Hz, $J_{\text{CdH}} = 4.9$ Hz, H_a), 3.959 (s, 6H, H_d), 3.592 (s, 9H, H_c). A crystal measuring $0.23 \times 0.18 \times 0.16$ mm³ was glued on the end of a glass fiber. The data were collected using the θ - 2θ technique over a θ range of 4.453 to 66.963°. The final data to parameter ratio was 10.51:1. Crystallographic data for **16** are provided in Table 1.

2.2.7. Other complexes investigated in this work

Winslow *et al.*²⁷ prepared two polymorphs of $[\text{Zn}(\text{L}_7)\text{Cl}_2]$ (**5**) by slow evaporation of an acetonitrile/methanol solution containing a 1:1 ratio of ZnCl_2 and L_7 . The crystal structure of the major polymorph (**5A**) was initially solved at 296 K while the minor polymorph (**5A**) was solved at 150 K. To allow for a more direct comparison of the two structures, the structure of **5A** was resolved at 150 K. Crystallographic data for **5A** and **5B** is provided in Table 2.

Winslow *et al.*²⁷ prepared $[\text{Cd}(\text{L}_7)(\text{NO}_3)_2]$ (**6**) by slow evaporation of an acetonitrile solution containing a 1:1 ratio of $\text{Cd}(\text{NO}_3)_2 \cdot 4\text{H}_2\text{O}$ and L_7 . ¹H NMR (CD_3CN , 3 mM): δ 8.656 (d, 2H, $^3J_{\text{HH}} = 5.4$ Hz, H_e), 7.921 (m, 2H, $^3J_{\text{HH}} = 7.8$ Hz, $^4J_{\text{HH}} = 1.7$ Hz, H_c), 7.539 (d, 2H, $^3J_{\text{HH}} = 7.9$ Hz, H_b), 7.465 (m, 2H, $^3J_{\text{HH}} = 5.4$ Hz, H_d), 4.175 (s, 4H, $^2J_{\text{SeH}} = 13.1$ Hz, H_a).

Winslow *et al.*²⁷ also prepared a cocrystal of 85% $[\text{Cd}(\text{L}_7)(\text{NO}_3)_2]$ (**6A**) and 15% $[\text{Cd}(\text{L}_2)(\text{NO}_3)_2]$ (**7A**) by slow evaporation of the filtrate obtained by vacuum filtration of precipitated **6** from a supersaturated acetonitrile solution obtained by mixing $\text{Cd}(\text{NO}_3)_2 \cdot 4\text{H}_2\text{O}$ and L_7 in a 1:1 ratio.²⁷ Although ¹H NMR of L_7 indicated only trace contamination with L_2 , this crystallization procedure inadvertently enhanced the relative concentration of L_2 leading to cocrystallization. The ¹H NMR spectrum of the cocrystalline material in CD_3CN had the expected sets of resonance for the **6** and **7A** in an approximate 85:15 ratio, indicating slow exchange on the ¹H chemical shift time scale.

Table 1. Crystallographic data for cocrystal of [Cd(L₇)(NO₃)₂] and [Cd(L₂)(NO₃)₂] (**6A,7A**), independent crystal of [Cd(L₂)(NO₃)₂] (**7B**) and [Cd(L₃)(NCCH₃)](ClO₄)₂ (**16**).

	6A,7A	7B	16
Empirical Formula	C ₁₂ H ₁₂ N ₄ O ₆ Se _{1.14} Cd	C ₁₂ H ₁₂ N ₄ O ₆ Se ₂ Cd	C ₁₇ H ₂₄ Cl ₂ N ₈ O ₈ Cd
Formula mass [g mol ⁻¹]	511.02	578.58	651.74
Crystal System	Triclinic	Triclinic	Trigonal
Space Group	P -1	P -1	R -3 c
<i>a</i> [Å]	8.0371(2)	8.06500(10)	12.2018(4)
<i>b</i> [Å]	8.4838(2)	8.51580(10)	12.2018(4)
<i>c</i> [Å]	12.9112(3)	13.8712(2)	57.998(2)
α [°]	80.8446(9)	80.1250(6)	90
β [°]	80.0131(9)	81.8550(6)	90
γ [°]	66.1735(8)	63.4800(5)	120
<i>V</i> [Å ³]	789.24(3)	837.509(19)	7478.1(6)
<i>Z</i>	2	2	12
Radiation (monochromatic)	Cu K α	Cu K α	Cu K α
λ [Å]	1.54178	1.54178	1.54178
<i>T</i> [K]	100(2)	100(2)	100(2)
ρ_{calcd} [Mg m ⁻³]	2.150	2.294	1.525
μ [mm ⁻¹]	14.475	15.786	9.522
R1 ^a , wR2 ^b [<i>I</i> > 2 σ (<i>I</i>)]	0.0391, 0.1260	0.0268, 0.0711	0.0727, 0.1714
R1 ^a , wR2 ^b (all data)	0.0394, 0.1261	0.0270, 0.0712	0.0764, 0.1275
GOOF	1.072	1.061	1.458

$$^a R1 = \frac{\sum ||F_o| - |F_c||}{\sum |F_o|}, \text{ and } S = \left[\frac{\sum [w(F_o^2 - F_c^2)^2]}{(n - p)} \right]^{1/2}$$

$$^b wR2 = \left[\frac{\sum [w(F_o^2) - (F_c^2)]^2}{\sum [w(F_o^2)^2]} \right]^{1/2}$$

Table 2. Crystallographic data for [Zn(L₇)Cl₂] polymorphs **5A** and **5B**.

	5A	5B
Empirical Formula	C ₁₂ H ₁₂ Cl ₂ N ₂ SeZn	C ₁₂ H ₁₂ Cl ₂ N ₂ SeZn
Formula mass [g mol ⁻¹]	399.47	399.47
Crystal System	Monoclinic	Tetragonal
Space Group	C 2/c	P4 ₃ 2 ₁ 2
<i>a</i> [Å]	23.6226(10)	8.92560(10)
<i>b</i> [Å]	8.4580(4)	8.92560(10)
<i>c</i> [Å]	16.2905(7)	18.4297(2)
α [°]	90	90
β [°]	121.2470(14)	90
γ [°]	90	90
<i>V</i> [Å ³]	2782.7(2)	1468.23(3)
<i>Z</i>	8	4
Radiation (monochromatic)	Cu K α	Cu K α
λ [Å]	1.54178	1.54178
<i>T</i> [K]	150(2)	150(2)
ρ_{calcd} [Mg m ⁻³]	1.907	1.807
μ [mm ⁻¹]	8.827	8.365
R1 ^a , wR2 ^b [<i>I</i> >2 σ (<i>I</i>)]	0.0320, 0.0934	0.0187, 0.0533
R1 ^a , wR2 ^b (all data)	0.0330, 0.0941	0.0188, 0.0533
GOOF	1.138	0.916

$$^a R1 = \sum | |F_o| - |F_c| | / \sum |F_o|, \text{ and } S = [\sum [w(F_o^2 - F_c^2)^2] / (n - p)]^{1/2}$$

$$^b wR2 = [\sum [w(F_o^2 - F_c^2)]^2 / \sum [w(F_o^2)^2]]^{1/2}$$

3. Results and Discussion

3.1. Carbonate-fixation by Cd(II) with less sterically demanding ligands

3.1.1. Preparation of less sterically demanding ligands

To complement previous studies of carbonate capture by Cd(II) complexes of **HL**₄ and **HL**₅, less sterically demanding amines **HL**₆ and **HL**₁ were targeted for Cd(II) coordination studies. Efforts to reproduce the established procedure³⁷ for synthesizing **HL**₆ were thwarted by apparent polymerization. Repeated synthetic attempts provided a highly viscous slightly gray-pink material in low yield with a broad featureless ¹H NMR spectrum. Attempted reaction of this material with Cd(ClO₄)₂·6H₂O in acetone or acetonitrile produced a highly insoluble white solid upon addition of Et₃N with indistinct ¹H NMR features. Carbonate bands were not detected through IR. Although an 8:1 mole ratio of diamine to ethylene sulfide was used to favor formation of **HL**₆, polymerization through reaction with both ends of the amine and disulfide formation upon exposure to trace amounts of air may have been occurring. Ethylenediamine was replaced by N,N-dimethylethylenediamine in further studies to avoid this problem.

In the first attempt to synthesized **HL**₁ from N,N-dimethylethylenediamine and ethylene disulfide, the procedure of Rose *et al.*³⁷ for making **HL**₆ was used. The goal of Rose's procedure was to minimize polymerization, however simplifying purification was more critical in the preparation of **HL**₁. Therefore, a new synthesis procedure was formed by combining elements from both Rose *et al.*³⁷ and the literature synthesis of **HL**₁.³⁸ Distillation provided **HL**₁ as confirmed by ¹H NMR. Although an unassigned impurity was evident in the ¹H NMR (δ_{H} 2.959 (t, ³J_{HH} = 6.55 Hz)), the ligand was sufficiently pure for further studies. In the absence of metal ions, **HL**₁ is highly air-sensitive. Solutions of **HL**₁ in air saturated solvents changed from colorless to yellow over time and the ¹H NMR spectrum changed significantly.

3.1.2. Cd(II) complex formation of HL₁ and ¹H NMR characterization

Complex **14** was successfully synthesized as a precipitate from CO₂-exposed solutions of HL₁, Cd(ClO₄)₂·6H₂O and triethylamine (NEt₃) in wet acetone. Elemental analysis supported formation of the hexanuclear bis-carbonate with less than 5% Et₃NHClO₄ contamination. NMR of the obtained precipitate (Fig. 7c-e) revealed some protons resonances were shifted downfield with respect to free ligand (Fig. 7a) consistent with the commonly observed deshielding influence of binding to Cd(II). The complex appearance of the peaks between 2.0-3.0 ppm was reminiscent of the ethylene ¹H NMR resonances observed for [(Cd(L₄))₆(μ₃-CO₃)₂](ClO₄)₂ (**1**). The ¹H NMR of **14** was unchanged over time. However, serial dilution over the concentration range of 7.4-0.13 mg/mL produced changes in the ¹H NMR of **15** (Fig. 7) suggesting an oligomerization process was occurring. The ¹H NMR of **1** did not change over a similar concentration range.

Air free preparation of “CdL₁ClO₄” (**15**) in ethanol/water was performed to permit investigation of bis-carbonate complex self-assembly using methods established by Lai *et al.*^{23,24} The heterogeneous isolate had much higher solubility in CD₃CN and CD₃NO₂ and contained L₁ based on ¹H NMR (Fig. 7 b). The preparation underwent a color change from pale yellow to purple and became a more homogeneous oil over time. The cause of these changes was not investigated.

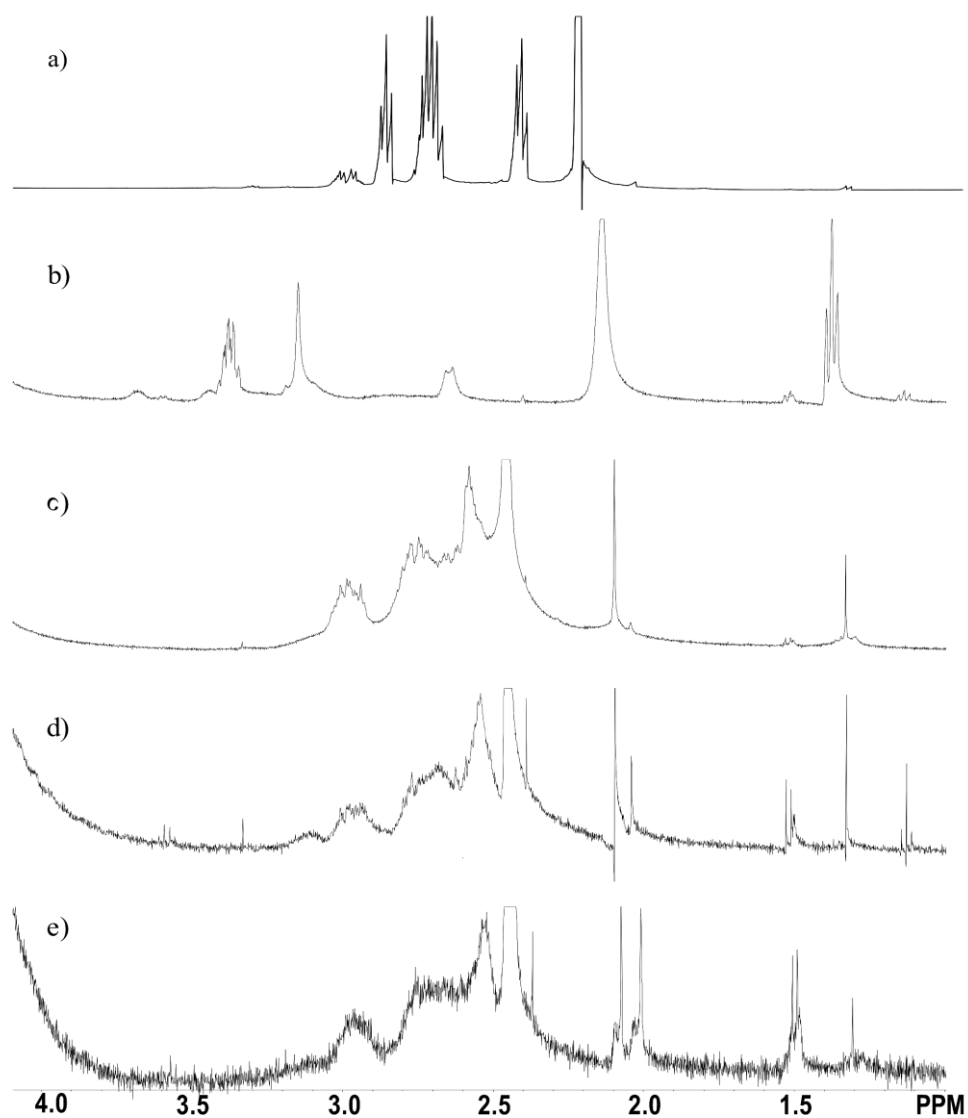


Figure 7. ^1H NMR spectra in CD_3NO_2 of a) **HL**₁, b) **15** (1.7 mg/mL), and **14** c) (7.4 mg/mL), d) (1.2 mg/mL), e) (0.13 mg/mL). Singlets are truncated to enhance lower intensity resonances.

3.1.3 IR characterization of **14** and **15**

Carbonate is associated with a strong IR band in the region $1400\text{--}1500\text{ cm}^{-1}$. It was not possible to assign specific bands in the IR spectrum of **1** to carbonate because **HL**₄ has significant infrared absorbance in this frequency range.²³ A modestly strong infrared absorbance in **HL**₁ also has a

relative infrared absorbance in this frequency range, the IR spectra of **14** and **15** were obtained for comparison.

Very strong IR bands around 1100 cm^{-1} were found for **15** (Fig. 8b). These are possibly associated with the C-O stretch (lit. $1150\text{-}1042\text{ cm}^{-1}$) of Cd(II) bound ethoxide formed from ethanol in the presence of the weak base Et_3N when activated by binding to the weak Lewis acid Cd(II). Also, the bands could be associated with ClO_4^- (lit. $1150\text{-}1050\text{ cm}^{-1}$). The intensity of the bands was so high that carbonate could be masked if present.

A complex series of IR bands was observed for **14** in the frequency range $1000\text{-}1700\text{ cm}^{-1}$. Detailed assignment of these features was not further pursued.

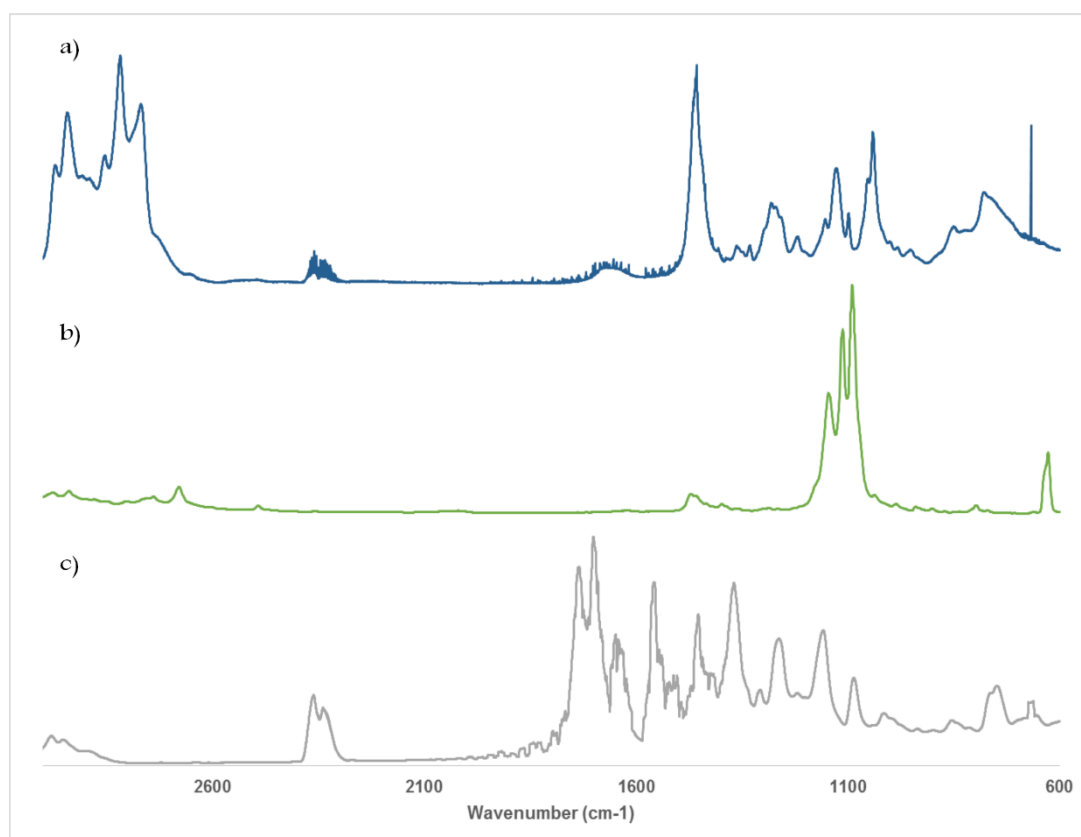


Figure 8. FTIR Spectra for a) **HL**₁, b) **15** and c) **14**.

3.1.3. ESI-MS characterization of **14** and **15**

As with complexes **1** and **2**, acetonitrile solutions of **14** and **15** had distinct ESI-MS speciation. The base peak for **14** (0.1 mg/mL in CH₃CN) was centered on m/z 840 (Fig. 9c,) and corresponded in part to $[(CdL_1)_6(CO_3)_2]^{2+}$ (Fig. 10) and there was also a large peak assigned to $[(CdL_1)_6(CO_3)_2(ClO_4)]^+$ centered on m/z 1777 (Fig. 9c). Interestingly, neither of these carbonate containing ions were observed in a 9.09 μ g/mL CH₃CN of **14**, suggesting the oligomeric bis-carbonated complexes are susceptible to dissociation to $[CdL_1]^+$ and carbonate when very dilute. Dilute acetonitrile solutions of **15** (0.15 mg/mL) were prepared using argon bubbled solvent. In the initial ESI-MS spectrum of **15**, the base peak was centered on m/z 978, which corresponded to $[(CdL_1)_3(ClO_4)_2]^+$ (Fig. 9a). None of the assigned ions in the ESI-MS spectrum of **15** contained carbonate.

Finally, *in situ* generation of **14** by the addition of CO₂ and Et₃N to **15** in acetonitrile was observed. To the argon purged acetonitrile solution of **15**, 1 μ L of Et₃N was added and then the solution was bubbled with CO₂ for 7 minutes. The ESI-MS spectra of **15**, now resembling that of **14**, had a new base peak at m/z 1777 that corresponded to $[(CdL_1)_6(CO_3)_2(ClO_4)]^+$ (Fig. 9b). This transformation occurred in minutes, providing the third documentation of rapid CO₂ fixation by a cadmium(II) complex.

3.1.4. Conclusions and future studies of CO₂ fixation with Cd(II)

Three different ligands providing an NN'S donor set have now been found to support the fixation of CO₂ by Cd(II). In this work, the sterically demanding pyridyl rings of **HL**₄ and **HL**₅ were replaced by a tertiary amine. This substitution still permitted carbon fixation by formation of a hexanuclear bis-carbonate complex. Based on solution state ¹H NMR studies and gas phase ESI-MS studies, **14** became increasingly unstable to dissociation with dilution.

Ongoing studies of **14** involve efforts to prepare crystals for X-ray crystallography. Ideally, crystalline material will have better resolved ^1H NMR spectra. In addition, alternative solvents will be used in the preparation of **15** to determine whether a more homogeneous material suitable for characterization by elemental analysis can be obtained.

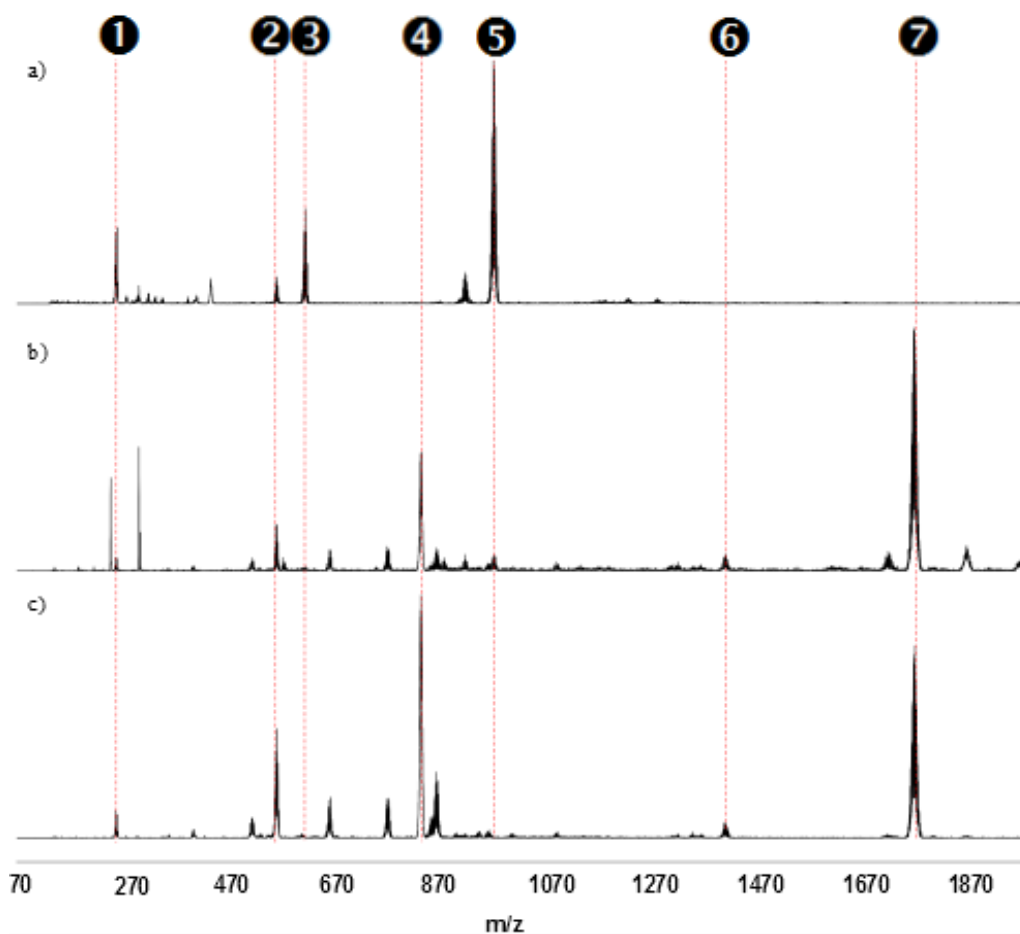


Figure 9. ESI-MS spectra for CH_3CN solutions of **15** (0.15 mg/mL) (a) originally, (b) with 1 μL of NEt_3 added and then bubbled with CO_2 for 7 min and (c) **14** (0.1 mg/mL). Selected assignments with m/z of the isotope distribution maximum are **1** 261 $[\text{CdL}_1]^+$, **2** 565 $[(\text{CdL}_1)_2(\text{C}_2\text{H}_5\text{O})]^+$, **3** 619 $[(\text{CdL}_1)_2(\text{ClO}_4)]^+$, **4** 840 $[(\text{CdL}_1)_6(\text{CO}_3)_2]^{2+}$, **5** 978 $[(\text{CdL}_1)_3(\text{ClO}_4)_2]^+$, **6** 1420 $[(\text{CdL}_1)_5(\text{CO}_3)_2]^+$ and **7** 1777 $[(\text{CdL}_1)_6(\text{CO}_3)_2](\text{ClO}_4)^+$.

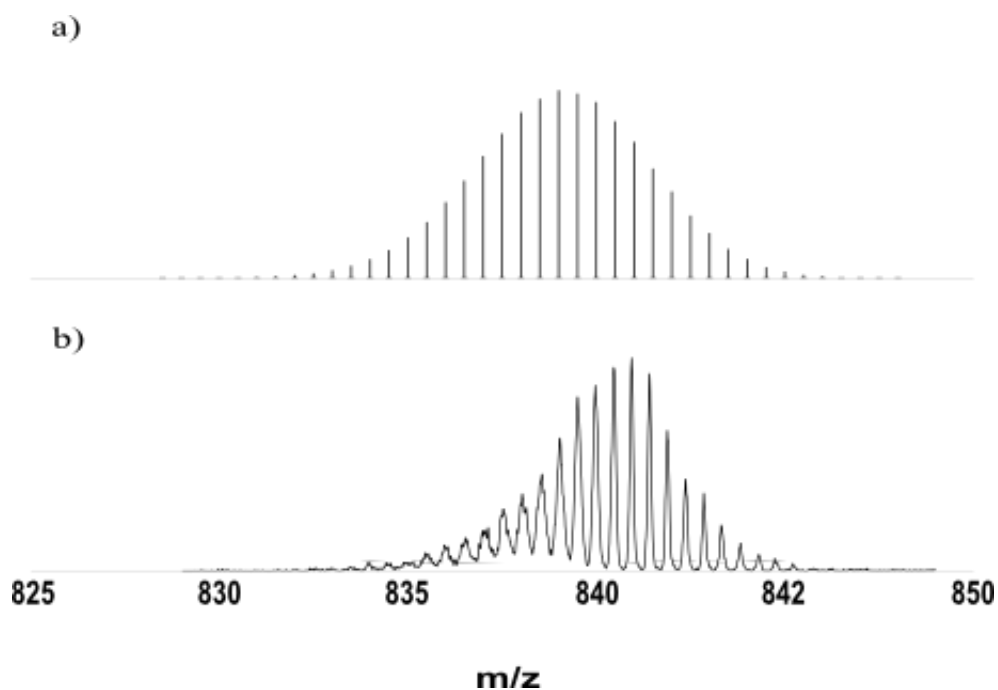


Figure 10. Calculated (a) and observed (b) isotope patterns for $[(\text{CdL}_1)_6(\text{CO}_3)_2]^{2+}$. The sharp, high intensity of peaks at the higher m/z side of this isotope distribution suggest an additional unidentified ion (base peak 840.92 m/z) with similar mass and +2 charge.

3.2 Group 12 metal ion coordination to neutral selenides

3.2.1. Preparation of \mathbf{L}_2

The potentially tridentate diselenide ligand \mathbf{L}_2 was prepared in a procedure very similar to that reported by Bhasin.³⁹ The reaction was conducted on a 16.0 mmol scale to provide \mathbf{L}_2 in 8.30% yield following column chromatography. The ligand was obtained in sufficient quantity and purity for the studies reported.

3.2.2. Structural comparison of $[\text{ZnL}_7\text{Cl}_2]$ polymorphs

Since there is precedent for formation of both macrocyclic³² and bicyclic³² metal ion complexes of \mathbf{L}_2 , some of the issues associated with macrocycle formation were investigated by comparing the crystal structures of $[\text{ZnL}_7\text{Cl}_2]$ polymorphs **5A** and **5B** (Fig. 11). The crystal structure of non-

symmetric **5A** was resolved at 150 K to allow for more direct comparison to the C_2 symmetric structure of **5B**. Figure 12 shows an overlay of the two structures. Selected bond lengths and bond angles are compared in Table 3. The metal center had distorted tetrahedral N_2Cl_2 coordination in both complexes. Significantly, the distance between Zn and Se was over 4.15 Å in the two complexes, above the sum of the van der Waals radii (Zn 2.10 Å and Se 1.90 Å).³¹ The differences between Zn-N, Zn-Cl and Se-C distances of the complexes were modest (Table 3). In both complexes the C-Se-C is the same and other bond angles are only modestly different.

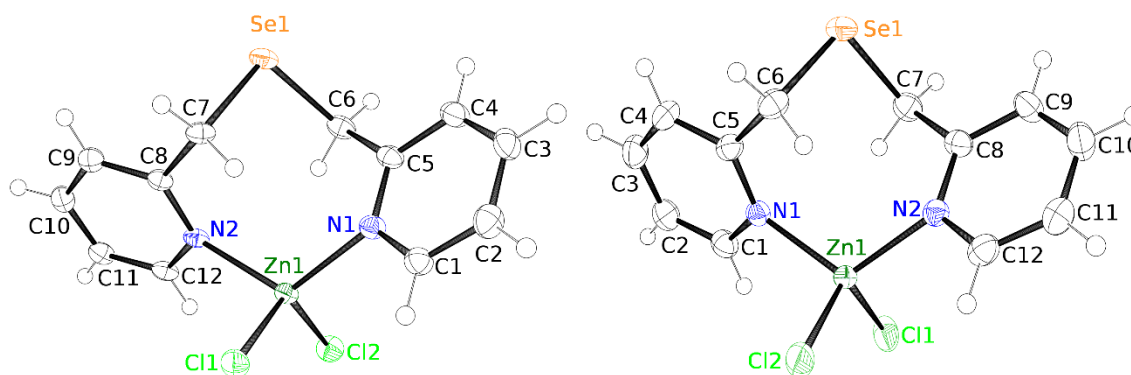


Figure 11. ORTEP diagram of [ZnL₇Cl₂] major polymorph (**5A**, left) and minor polymorph (**5B**, right) with thermal ellipsoids at 50% level.

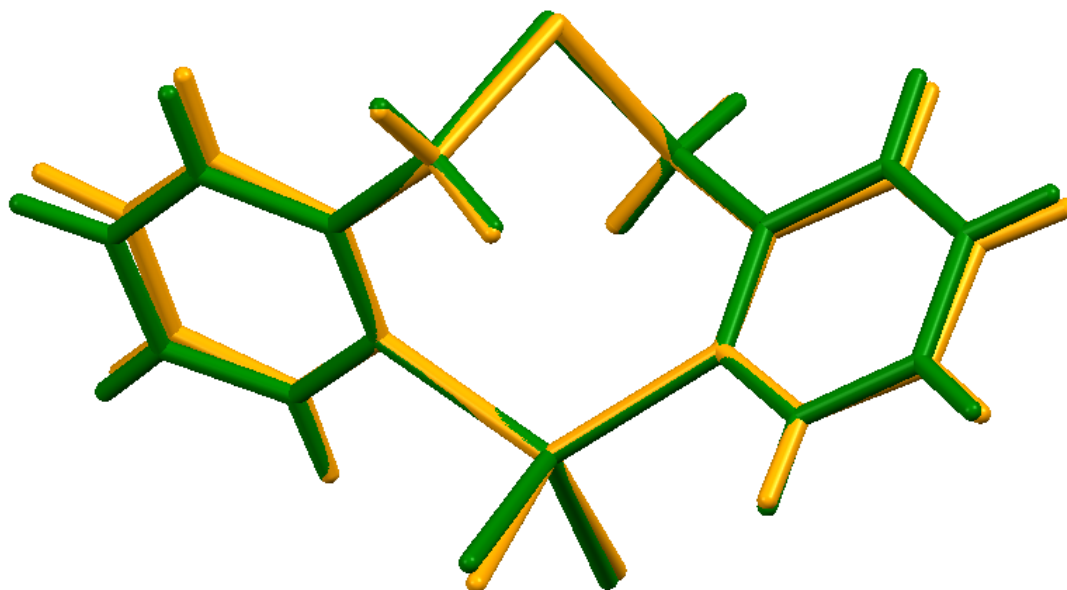


Figure 12. Structural overlay of **5A** (green) and **5B** (orange) based on alignment of Zn, N1 and N2. Root mean square (rms) deviation of overlaid atom positions is 0.00942 Å.

Table 3. Selected bond distances (Å) and angles (°) in [Zn(L₇)Cl₂] polymorphs **5A** and **5B**.

5A		5B ^a	
Zn(2)-N(2)	2.054(3)	Zn(1)-N(1)	2.056(2)
Zn(2)-N(1)	2.074(3)		
Zn(2)-Cl(2)	2.2312(9)	Zn(1)-Cl(1)	2.2324(7)
Zn(2)-Cl(1)	2.2295(9)		
Se(1)-C(6)	1.966(3)	Se(1)-C(6)	1.965(3)
Se(1)-C(7)	1.975(3)		
C(6)-Se(1)-C(7)	98.25(13)	C(6)-Se(1)-C(6)#1	98.41(15)
N(2)-Zn(2)-N(1)	117.17(11)	N(1)#1-Zn(1)-N(1)	116.97(12)
N(2)-Zn(2)-Cl(2)	103.71(8)	N(1)#1-Zn(1)-Cl(1)	105.82(5)
N(1)-Zn(2)-Cl(2)	101.97(8)	N(1)-Zn(1)-Cl(1)	105.50(6)
N(2)-Zn(2)-Cl(1)	108.58(8)	N(1)#1-Zn(1)-Cl(1)#1	105.51(6)
N(1)-Zn(2)-Cl(1)	105.11(8)	N(1)-Zn(1)-Cl(1)#1	105.82(5)
Cl(2)-Zn(2)-Cl(1)	120.92(4)	Cl(1)-Zn(1)-Cl(1)#1	117.82(5)

^a Symmetry transformations used to generate equivalent atoms: #1 -y+1,-x+1,-z+3/2

The polymorphs had clear differences in packing. As shown in Figure 13, in the crystal the N1 pyridyl rings of **5A** are oriented for a displaced parallel π - π stacking interaction with a centroid distance of 3.808 Å. In contrast, the pyridyl rings of adjacent molecules in the minor polymorph **5B** are not parallel or otherwise oriented for optimum π - π stacking interaction in the crystal

structure (Fig. 14). Significantly, the density of major isomer **5A** is 0.1 Mg m^{-3} higher than that of **5B** (Table 1). Higher density is a common feature of more stable polymorphs.

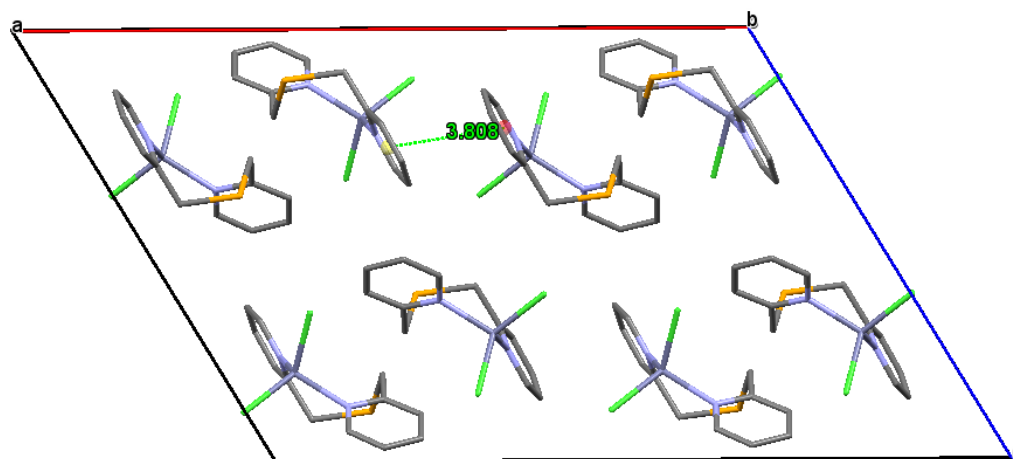


Figure 13. Packing diagram for **5A**, viewed down the b-axis.

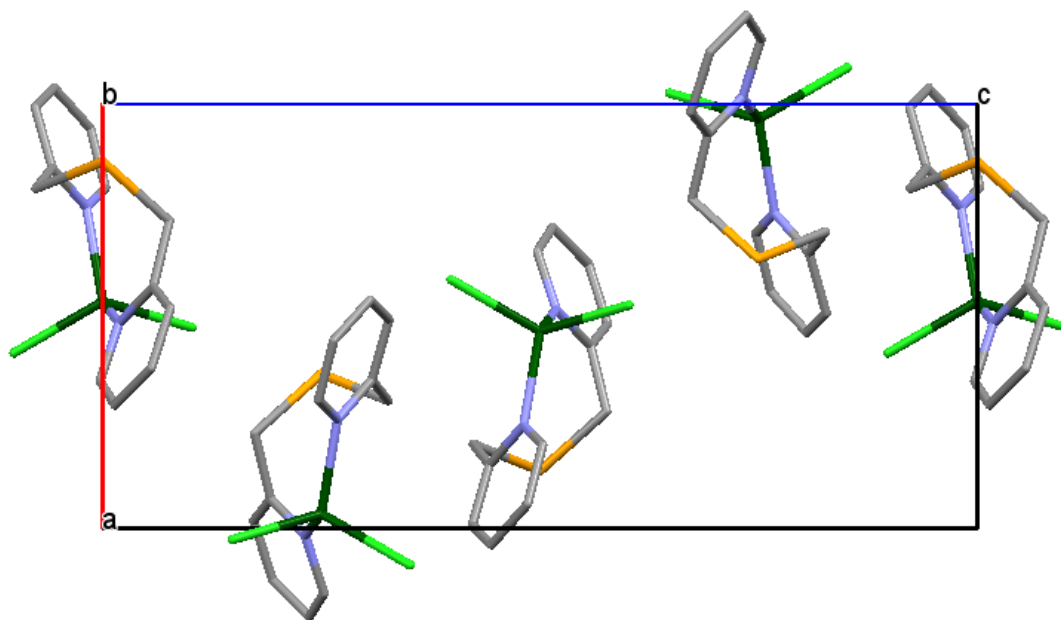


Figure 14. Packing diagram for **5B**, viewed down the b-axis.

Although both **5A** and **5B** were macrocyclic with no Zn-SeR₂ binding, the CdCl₂ complex of **L₇** was bicyclic and had a Cd-SeR₂ bond distance of 2.892 Å,²⁷ within the sum of the van der Waals radii. The Cd(II) complex crystallized as a chloride-bridged dimer with approximately octahedral coordination. The ligand was bound in a facial manner with the Cd(II) significantly displaced from the N1-N2-Se plane, while in both **5A** and **5B** the metal ion was nearly coplanar with the heteroatoms of the ligand.

3.2.3. Preparation and structural characterization of [CdL₂(NO₃)₂] (**7B**)

The complex **7B** was prepared from 1:1 acetonitrile solutions of Cd(NO₃)₂·4H₂O and **L₂** as both a precipitate and a crystalline material. Colorless X-ray quality crystals were recovered in very low yield. The precipitate was more highly colored than expected for a complex of Cd(II), but provided a satisfactory elemental analysis. Proton NMR characterization of **7B** confirmed tentative resonance assignments for the minor component of the **6,7A** co-crystalline material isolated recently (Fig. 15). Protons of **L₂** were deshielded by 0.16–0.80 ppm in **7B** with respect to free ligand through σ donation to Cd(II). The coupling constant between the methylene protons and ⁷⁷Se changed from 15.3 Hz in **L₂** to 17.8 Hz in **7B**. Confirming the NMR properties of **7B** complex helped shed light on the mystery of **6** and **7A** cocrystallization from **L₇** containing insufficient **L₂** for detection by NMR. Proton NMR of the precipitate removed in high yield prior to slow evaporation bore no sign of the methylene resonance for **7A** at 4.216 ppm. Hence, precipitation selectively removed **6**. As a result **L₂** became concentrated in the filtrate used for crystallization therefore making cocrystallization favorable.

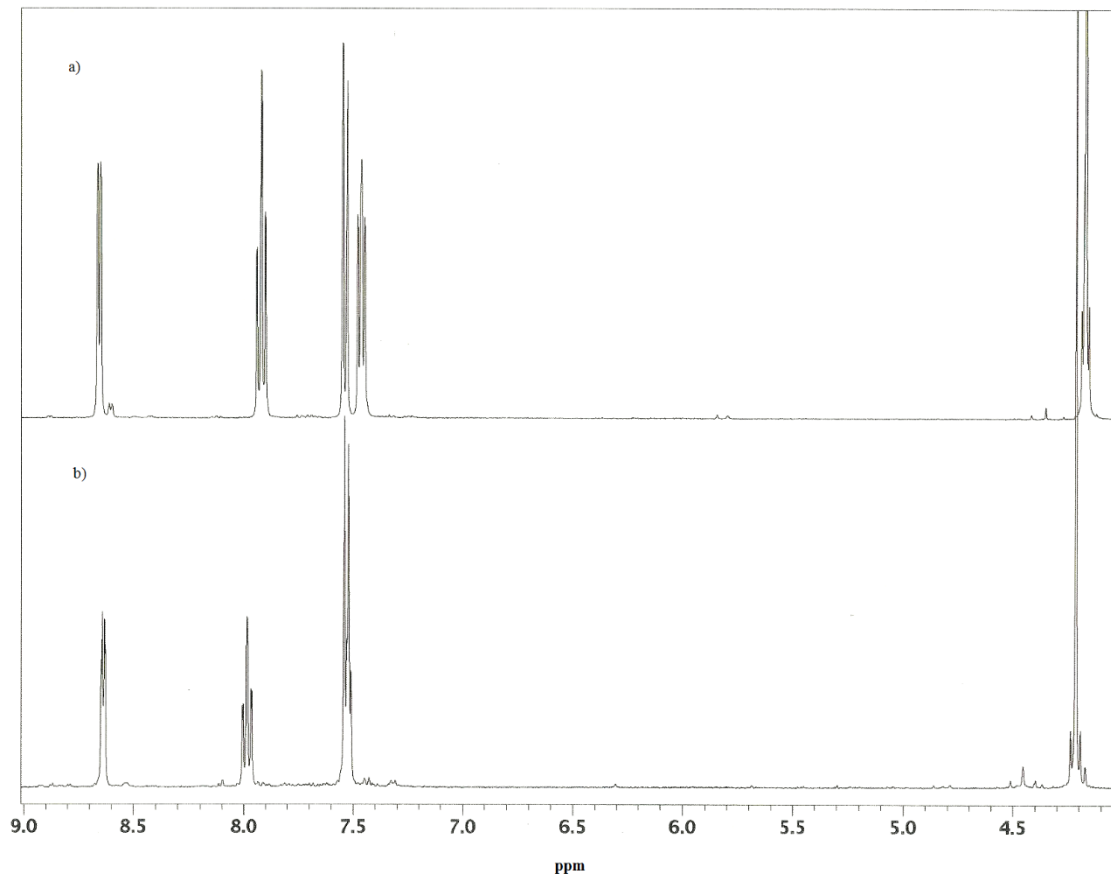


Figure 15. ^1H NMR spectra of a) **6** and b) **7B**.

As shown in Figure 16, the metal center of **7B** has distorted pentagonal bipyramidal coordination. Selected bond lengths and angles for **7B** are shown in Table 4 and Table 5, respectively. The two pyridyl nitrogens are in the axial positions with an average Cd-N distance of 2.289 (16) Å with a N-Cd-N bond angle of 159.10(10)°. The selenium and four nitrate oxygen occupy the equatorial plane. The average Cd-O bond distance was 2.426 (69) Å. Significantly, the Cd-Se distance was 2.898 Å, within the sum of the van der Waals radii (Cd 2.20 Å and Se 1.90 Å).³¹

Table 4. Selected bond distances (\AA) in **6**, **7A** and **7B**.

6, 7A		7B	
Cd(1)-N(1)	2.257(5)	Cd-N(1)	2.301(3)
Cd(1)-N(2)	2.262(5)	Cd-N(2)	2.278 (3)
Cd(1)-O(4)	2.326(5)	Cd(1)-O(5)	2.332(3)
Cd(1)-O(2)	2.373(5)	Cd(1)-O(2)	2.424(3)
Cd(1)-O(5)	2.461(5)	Cd(1)-O(1)	2.452(3)
Cd(1)-O(1)	2.516(5)	Cd(1)-O(4)	2.495(3)
Cd(1)-Se(1)	2.8526(9)	Cd(1)-Se(1)	2.8979(4)
Cd(1)-Se(2)	3.033(6)	Se(1)-Se(2)	2.3127
Se(2)-Se(3)	2.314(10)		

Table 5. Selected angles (°) in **6**, **7A** and **7B**.

6, 7A		7B	
N(1)-Cd(1)-N(2)	151.9(2)	N(2)-Cd(1)-N(1)	159.10(10)
N(1)-Cd(1)-O(4)	107.59(19)	N(2)-Cd(1)-O(5)	104.07(10)
N(2)-Cd(1)-O(4)	99.89(19)	N(1)-Cd(1)-O(5)	96.71(10)
N(1)-Cd(1)-O(2)	96.49(19)	N(2)-Cd(1)-O(2)	99.62(10)
N(2)-Cd(1)-O(2)	94.36(19)	N(1)-Cd(1)-O(2)	87.53(10)
O(4)-Cd(1)-O(2)	78.42(17)	O(5)-Cd(1)-O(2)	75.57(10)
N(1)-Cd(1)-O(5)	90.58(18)	N(2)-Cd(1)-O(1)	88.11(9)
N(2)-Cd(1)-O(5)	101.44(18)	N(1)-Cd(1)-O(1)	80.71(9)
O(4)-Cd(1)-O(5)	53.74(17)	O(5)-Cd(1)-O(1)	127.98(9)
O(2)-Cd(1)-O(5)	131.34(16)	O(2)-Cd(1)-O(1)	52.45(9)
N(1)-Cd(1)-O(1)	84.11(17)	N(2)-Cd(1)-O(4)	87.53(10)
N(2)-Cd(1)-O(1)	82.21(18)	N(1)-Cd(1)-O(4)	103.59(9)
O(4)-Cd(1)-O(1)	130.63(16)	O(5)-Cd(1)-O(4)	52.95(9)
O(2)-Cd(1)-O(1)	52.36(16)	O(2)-Cd(1)-O(4)	128.01(9)
O(5)-Cd(1)-O(1)	174.03(16)	O(1)-Cd(1)-O(4)	175.61(8)
N(1)-Cd(1)-Se(1)	77.56(14)	N(2)-Cd(1)-Se(1)	91.87(7)
N(2)-Cd(1)-Se(1)	78.05(15)	N(1)-Cd(1)-Se(1)	73.04(7)
O(4)-Cd(1)-Se(1)	139.12(13)	O(5)-Cd(1)-Se(1)	128.89(7)
O(2)-Cd(1)-Se(1)	142.29(12)	O(2)-Cd(1)-Se(1)	149.49(7)
O(5)-Cd(1)-Se(1)	86.26(12)	O(1)-Cd(1)-Se(1)	100.29(6)
O(1)-Cd(1)-Se(1)	89.92(11)	O(4)-Cd(1)-Se(1)	80.31(6)
N(1)-Cd(1)-Se(2)	91.5(2)	C(6)-Se(1)-Se(2)	100.30(11)
N(2)-Cd(1)-Se(2)	65.3(2)	C(6)-Se(1)-Cd(1)	83.06(10)
O(4)-Cd(1)-Se(2)	131.75(19)	Se(2)-Se(1)-Cd(1)	102.279(15)
O(2)-Cd(1)-Se(2)	144.27(16)	C(7)-Se(2)-Se(1)	101.10(10)
O(5)-Cd(1)-Se(2)	83.12(16)		
O(1)-Cd(1)-Se(2)	94.27(15)		
C(6)-Se(1)-C(7)	100.5(3)		
C(6)-Se(1)-Cd(1)	83.1(2)		
C(7)-Se(1)-Cd(1)	84.2(2)		
C(7)-Se(2)-Se(3)	91.6(4)		
C(7)-Se(2)-Cd(1)	83.6(3)		
Se(3)-Se(2)-Cd(1)	103.2(3)		
C(6)-Se(3)-Se(2)	87.5(4)		

Motivations to prepare **7B** included curiosity as to whether a macrocyclic or bicyclic complex would form. Co-crystallization of **6** with **7A** was serendipitous. The structural solution of the co-crystalline material had coincident locations for all non-selenium atoms of the two species. Since there is precedent for both macrocyclic binding of **L₂** to metal ions without M-(Se₂R₂) coordination and bicyclic binding of **L₂** to metal ions with M-(Se₂R₂) coordination, independent preparation of **7** was necessary to determine whether the lattice of **6** was necessary to form Cd-(Se₂R₂) bond. As shown in Figure 17, the structures of **7A** and **7B** are similar. Interestingly, the Cd-(Se₂R₂) bond distance in **7A** was 3.033 Å,²⁷ 0.135 Å longer than found in **7B**. The conformations of the more rigid five-membered chelate rings were nearly identical while the side of the six-membered chelate ring far from the metal ion had more sizable differences in atom positions. As shown in Figure 18, in the structures of **7A** and **7B** there are displaced parallel π - π stacking interactions between N1-N1 pyridyl and N2-N2 pyridyl rings.

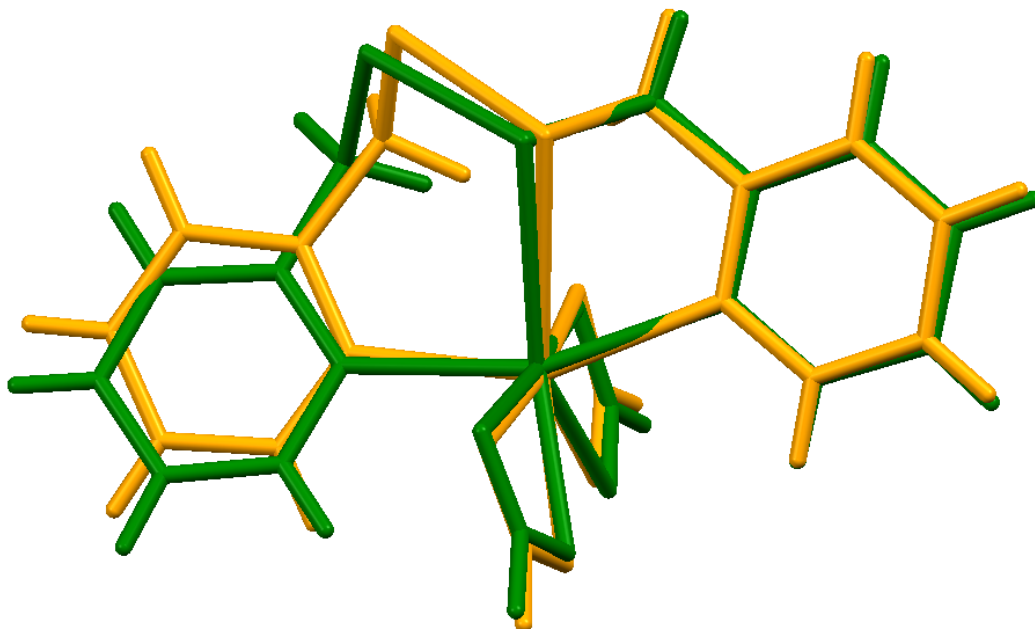


Figure 17. Structural overlay of **7A** (orange) and **7B** (green) based on alignment of Cd-Se-C-N chelate rings. Root mean square (rms) deviation in overlaid atom positions is 0.149 Å.

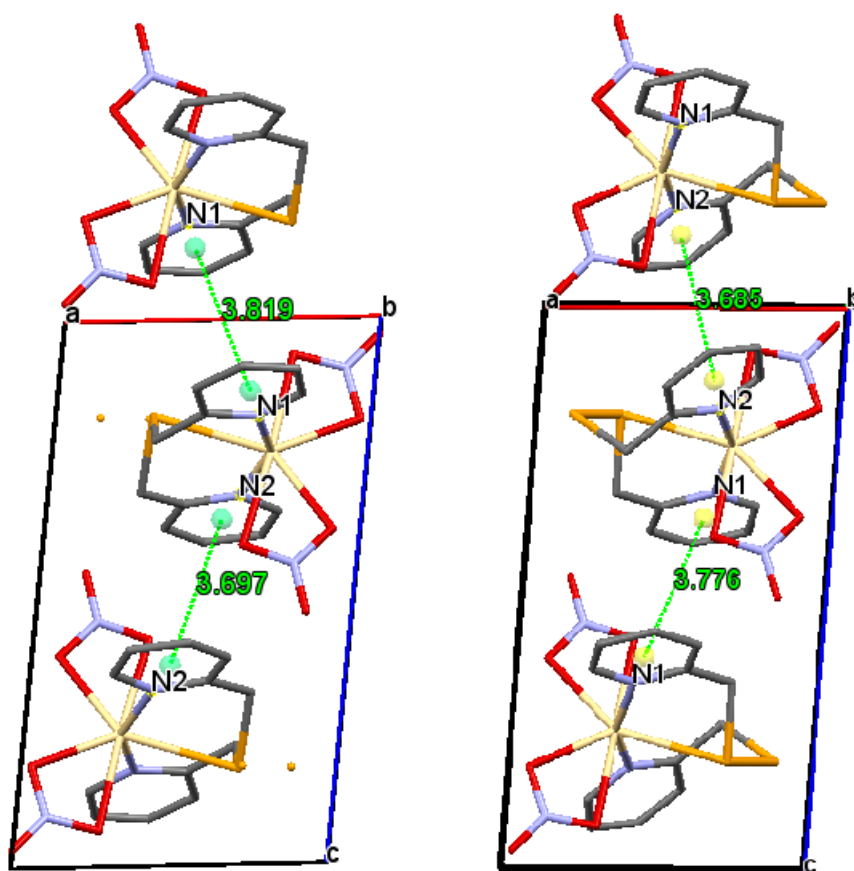


Figure 18. Packing diagrams for **7A** (left) and **7B** (right) highlighting π - π stacking.

Based on a search of the Cambridge Crystallographic Database (v. 5.32 updated Nov 2013), only seven mononuclear complexes with $M-(Se_2R_2)$ bonds complexes with five different metal ions have been structurally characterized previously (Table 6).^{35, 40-42} Table 6 is organized according to the observed M-Se bond distance, $d(M-Se)$. In general, the larger, softer metal ions had longer M-Se bond distances that were closer to the sum of the van der Waals radii of the metal and Se ($\Sigma r_v(MSe)$). As also noted in Table 6, there is generally an inverse relationship between the Se-Se bond distance, $d(Se-Se)$, and $d(M-Se)$. The variants of **7** have longer M-Se bonds than all the other structurally characterized mononuclear diselenide complexes. This is to be expected since cadmium has a larger van der Waals radius than the other metals listed in Table 6.

Table 6. Overview of structurally characterized mononuclear complexes with M-(Se₂R₂) bonds.

Metal	Hardness	r _v (M) ^{31,a}	Σ r _v (MSe)	d (M-Se)	% Σ r _v (MSe) ^j	d (Se-Se)
Fe(II)	Borderline	2.05	3.95	2.424 ^b	61.4	2.411
Ir(III)	Borderline	2.00	3.09	2.451 ^c	62.9	2.370
Cr(II)	Borderline	2.05	3.95	2.524 ^d	63.9	2.372
				2.545 ^e	64.4	2.327
Cu(II)	Borderline	2.00	3.90	2.622 ^f	67.2	2.318
W(II)	Soft	2.10	4.00	2.648 ^g	67.9	2.368
				2.671 ^h	66.8	2.330
Cd(II)	Soft	2.20	4.10	2.898 ⁱ	70.7	2.313
				3.033 ⁱ	74.0	2.314

^a All measurements are in Å; r_v = van der Waals radii. ^b ref 40. ^c ref 41. ^d ref 42. ^e ref 42. ^f ref 32. ^g ref 42. ^h ref 42. ⁱ This work. ^j % Σ r_v (MSe) = (d(M-Se)/ Σ r_v (MSe))*100. Free ligand d(Se-Se) = 2.2969(9) Å⁴³.

3.2.4. Conclusions and future studies of Group 12 metal ion coordination to neutral selenides

Prior to recent studies in the Bebout laboratory, crystallographic documentation for bonding between neutral selenide ligands and both Zn(II) and Cd(II) was unavailable. Potentially tridentate ligands with N₂Se donor groups have now provided the first three examples of CdSeR₂ bonds, the first ZnSeR₂ bond and the first Cd-(Se₂R₂)bond. Ligands of the type investigated in this work have both macrocyclic and bicyclic coordination modes. They also have the flexibility to bind in either a facial manner with the metal well outside the plane formed by the three donor atoms or a meridional manner in which the metal lies very close to the plane containing the chelating atoms. Using perchlorate, chloride and nitrate counterions, a structurally diverse series of Zn(II) and Cd(II) complexes of **L**₇ has been characterized.

These solid state studies will be complemented by solution state NMR studies. While divalent Group 12 metal ions are generally spectroscopically silent d¹⁰ metal ions, ¹¹¹Cd and ¹¹³Cd have 12.80% and 12.22% natural abundance, respectively, and spin *I* = ½, making them reasonably

sensitive for NMR studies. Variable temperature ^{77}Se NMR (7.63% natural abundance, $I = 1/2$) or ^{113}Cd NMR can potentially be used to characterize bonding interactions between cadmium and selenium in solution. Bonding interactions exceeding the $^1J_{\text{CdSe}}$ time scale will result in coupling satellites around the main resonance. Although the theory for heteronuclear coupling involving heavy metal ions is poorly developed, due to relativistic effect $^1J_{\text{CdSe}}$ are expected to be larger than $^1J_{\text{CdC}}$ which are typically around 100 Hz. To detect heteronuclear coupling, the lifetime of the interaction must exceed the frequency of the coupling interaction. The Cd(II) complexes associated with this work are promising candidates for reporting the first heteronuclear coupling between Cd and Se. Since dietary SeMet is commonly integrated into proteins, which have a rich abundance of metal binding groups, estimated solution lifetimes for Cd-SR₂ interactions in chelating environments are potentially relevant to developing a better understanding of physiologically relevant Cd(II) and selenium chemistry.

3.3. α/δ -Carbonic Anhydrase modeling with multidentate imidazolyl ligands

3.3.1. Structural characterization of $[\text{Cd}(\text{L}_3)(\text{NCCH}_3)](\text{ClO}_4)_2$ (**16**)

Complex **16** was prepared by slow evaporation of an acetonitrile/toluene solution containing a 1:1 ratio of $\text{Cd}(\text{ClO}_4)_2 \cdot 6\text{H}_2\text{O}$ and **L**₃. The coordination sphere of Cd(II) has three-fold symmetry in **16** (Fig. 19). Selected bond lengths and angles for **16** are shown in Table 7. The ligand is tetradentate with the acetonitrile bound *trans* to the tertiary amine nitrogen. The Cd-N bond distances to the crystallographically identical imidazolyl ring nitrogens and the acetonitrile nitrogen are nearly the same while the distance to the tertiary amine nitrogen is over 0.3 Å longer. The Cd(II) ion is displaced from plane formed by the imidazolyl nitrogens towards the acetonitrile ligand, resulting in a tertiary amine capped tetrahedral coordination geometry. The N-Cd-N bond for the tetrahedrally arranged nitrogens range from 106.37(19) to 112.39(17) Å. In Figure 20 displaced π - π stacking interactions between the imidazolyl moieties of adjacent molecules of **16** is shown.

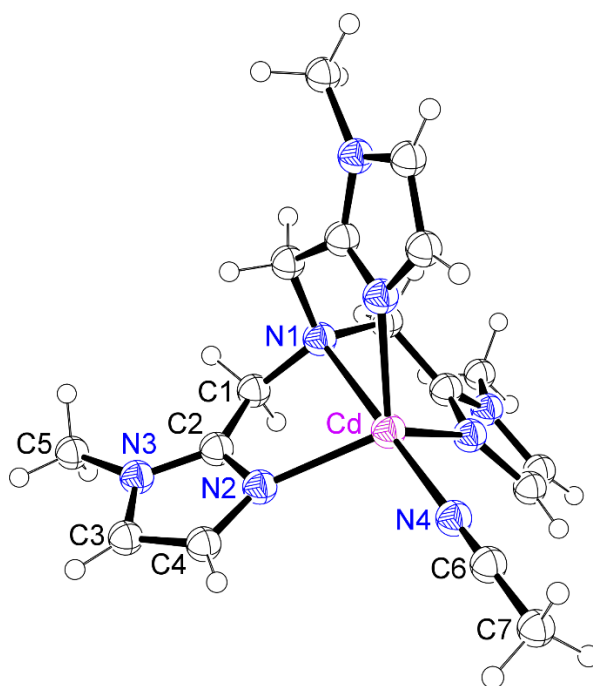


Figure 19. ORTEP diagram of $[\text{CdL}_3(\text{NCCH}_3)]^{2+}$ with thermal ellipsoids at 50% level. The molecule was only 1/3 independent in the crystal structure.

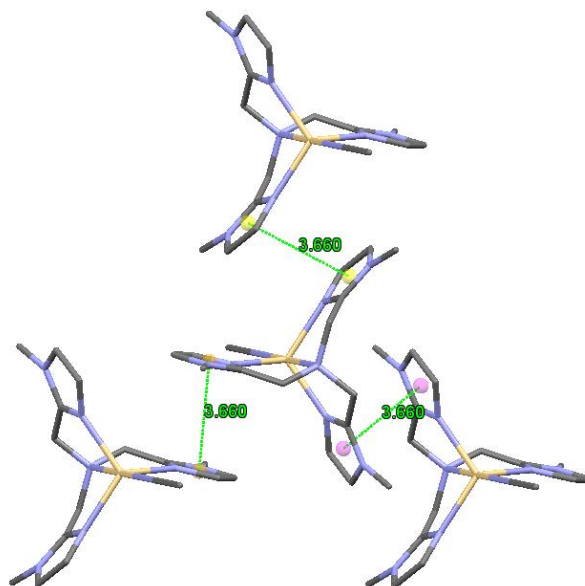


Figure 20. Packing diagram for $[\text{CdL}_3(\text{NCCH}_3)]^{2+}$ in **16** highlighting π - π stacking.

Table 7. Selected bond distances (Å) and angles (°) in **16**.

16^a	
Cd-N(1)	2.535(13)
Cd-N(2)	2.210(8)
Cd-N(4)	2.228(15)
N(2)-Cd-N(1)	73.63(19)
N(2)-Cd-N(2)	112.39(17)
N(2)-Cd-N(4)	106.37(19)
N(1)-Cd-N(4)	180.0
C(6)-N(4)-Cd(1)	180.0

^aSymmetry transformations used to generate equivalent atoms: #1 -y+1,x-y,z #2 -x+y+1,-x+1,z #3 -x+2/3,-x+y+1/3,-z+5/6 #4 -x+y,-x,z #5 -y,x-y,z #6 -x,-y,-z+1

The only complexes of **L**₃ structurally characterized previously involve Mn(II)³³, Fe(III)³, Cu(II)³⁴ and Hg(II)³⁵ (CCDC v. 5.32 updated Nov 2013). Although no complexes of Zn(II) with **L**₃ have been reported, there are a wide variety of derivatized variants of **L**₃ with structurally characterized Zn(II) complexes. The isostructural complex of Hg(II) (**12**) has comparable M-N bond lengths with the imidazolyl nitrogens, but the tertiary amine is 0.107 Å further from the metal ion. In addition, the Cd-N bond with acetonitrile is 0.036 Å shorter than its Hg-N counterpart. Interestingly, **12** was stable for an extended period of time but the isolated crystals of **16** became opaque overnight. Based on elemental analysis, the acetonitrile of **16** was replaced by adventitious water from the atmosphere. Interestingly, substitution of acetonitrile by a water molecule enhances parallels with the metal coordination of Zn(II) in the active site of wild-type HCAB.

The coordination of Cd(II) in complex **16** is remarkably similar to the coordination of Zn(II) by HCAB. In the refined structure of Zn(II)HCAB (PDB entry: 1CA2), the distances between Zn(II) and the metal-binding residues (N_{ϵ_2} of His 94, N_{ϵ_2} of 96, and N_{δ_1} of His 119) are 2.0 Å, 2.1 Å and 1.9 Å, respectively.⁴⁴ A water oxygen completes the tetrahedral coordination of Zn(II) with a Zn-O separation of approximately 2.1 Å. The N-Zn-N angles range between 101.6 – 113.5°. The Cd-N bond distances are slightly longer in **16**, as expected for binding to a metal ion with larger van der Waals radius.

The preservation of the three-fold symmetry in complex **16** and the equivalency of the methylene protons could be observed by ¹H NMR in CD₃CN solution (Fig. 21). Complex **16** exhibited a single set of proton resonances for each type of ligand proton. Heteronuclear coupling was observed between ^{111/113}Cd and both H_a and H_b with a coupling constant of 4.9 Hz. Stronger heteronuclear coupling between ¹⁹⁹Hg and these protons was observed in **12**, as expected due to greater relativistic contributions.

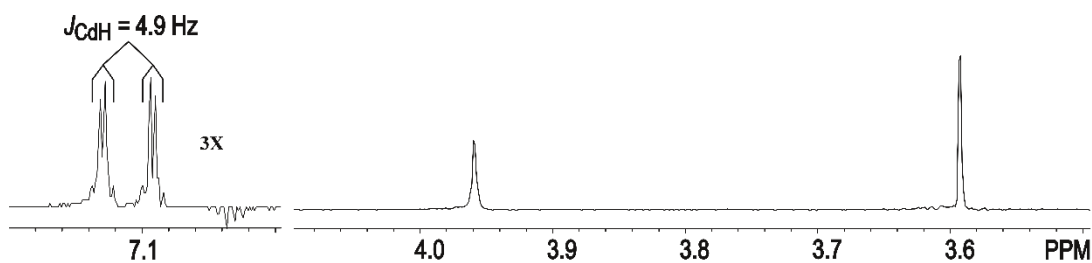


Figure 21. ¹H NMR spectra of **16**. The region of the coupling constant has been zoom in three-fold (3X).

3.3.2. Conclusions and future directions for carbonic anhydrase modeling

Although **L**₃ is constructed from 2-alkyl substituted imidazolyl rings rather than 4-alkyl substituted imidazolyl rings that resemble histidine more closely, coordination of Cd(II) in **16** bore extensive similarity to the metal binding site of Zn(II)HCAB. Future studies may involve efforts to prepare a structurally characterized complexes of Zn(II) with **L**₃ for comparison to **12** and **16**. In addition, it would be very interesting to investigate whether any of the complexes of **L**₃ were capable of performing biomimetic carbon dioxide hydration chemistry.

4. Conclusion

The recent discovery of a biologically beneficial role for Cd(II) has motivated further investigation of its coordination chemistry. The synthesis and characterization of Cd(II) complexes in a 1:1 ratio with **HL**₁, **L**₂, and **L**₃ has contributed to a better understanding of potentially biologically relevant interactions between Cd(II) and imidazoles, thiolates, selenoethers and diselenides. One common theme in the studies reported is the unusual versatility of multidentate chelating ligands.

The synthesis and characterization of complex **14** expanded the series of complexes between Cd(II) and NN'S tridentate ligands with CO₂ fixing properties to a ligand without aromatic nitrogen donors. Despite the absence of rigid pyridyl rings in **HL**₁ like those found in **HL**₄ and **HL**₅, a self-assembled (CdS)₆(μ₃-CO₃)₂ was observed through ESI-MS experiments and supported by elemental analysis. This result will help expand the foundation for understanding Cd(II)-associated bioactivity in carbonic anhydrases and inspire new strategies for CO₂ fixation.

Although selenium has been associated with physiological processing of Cd(II), the coordination chemistry of Cd(II) with neutral selenides has not been extensively investigated. The

synthesis and characterization of complex **7B** confirmed Cd-(Se₂R₂) bond formation could be fostered by a chelating ligand. Further studies will address the lifetime of interactions between Cd(II) and diselenides in solution.

Finally, the synthesis of **16** has demonstrated the efficiency of structurally modeling histidine-containing active sites with L₃. The coordination environment of Cd(II) in complex **16** was highly similar to the coordination of Zn(II) in HCAB. Additional parallels between **16** and HCAB include interchangeable occupancy of the fourth tetrahedral ligand site. Future studies will investigate whether **16** catalyzes carbon dioxide hydration.

References

- [1] Andreini, C., Bertini, I., Cavallaro, G., Holliday, G. L., Thornton, J. M., “Metal ions in biological catalysis: from enzyme databases to general principles” *J. Biol. Inorg. Chem.* **2008**, *13*, 1205-1218.
- [2] Waldron, K. J., Rutherford, J. C., Ford, D., Robinson, N. J., “Metalloproteins and metal sensing” *Nature* **2009**, *460*, 823-830.
- [3] Cheruzel, L. E., Wang, J., Mashuta, M. S., Buchanan, R. M., “Structure and properties of an Fe(III) complex containing a novel amide functionalized polyimidazole ligand” *Chem. Commun.* **2002**, 2166-2167.
- [4] Winer, B. Y., Berry, S. M., Pike, R. D., Bebout, D. C., “Synthesis of bis(2-pyridylmethyl)selenide and solid-state structural characterization of bis-tridentate zinc triad perchlorate chelates” *Polyhedron* **2012**, *48*, 125-130.
- [5] Summers, M. F., “Cadmium-113 NMR spectroscopy of coordination compounds and proteins” *Coord. Chem. Rev.* **1988**, *86*, 43-134.
- [6] Lane, T. W., Morel, F. M. M., “A biological function for cadmium in marine diatoms” *Proc. Natl Acad. Sci.* **2000**, *97*, 4627-4631.
- [7] Bouroushian, M., “Electrochemistry of metal chalcogenides” *Springer-Verlag Berlin Heidelberg*, **2010**.
- [8] Weekley, C. M., and Harris, H. H., “Which form is that? The importance of selenium speciation and metabolism in the prevention and treatment of disease” *Chem. Soc. Rev.* **2013**, *42*, 8870-8894.
- [9] Doney, S. C., Bopp, L., Long, M. C., “Historical and future trends in ocean climate and biogeochemistry” *Oceanography* **2014**, *27*, 108-119.

- [10] van Vuuren, D. P., Edmonds, J., Kainuma, M., Riahi, K., Thomson, A., Hibbard, K., Hurtt, G. C., Kram, T., Krey, V., Lamarque, J. F. and others, "The representative concentration pathways: an overview" *Climatic Change* **2011**, *109*, 5-31.
- [11] Alterio, V., Langella, E., Viparelli, F., Vullo, D., Ascione, G., Dathan, N. A., Morel, F. M. M., Supuran, C. T., De Simone, G., Monti S. M., "Structural and inhibition insights into carbonic anhydrase CDCA1 from the marine diatom *Thalassiosira weissflogii*" *Biochimie* **2012**, *94*, 1232-1241.
- [12] Lane, T. W., Morel, F. M. M., "Regulation of carbonic anhydrase expression by zinc, cobalt, and carbon dioxide in the marine diatom *Thalassiosira weissflogii*" *Plant Physiology* **2000**, *123*, 345-352.
- [13] Lane, T., Saito, M. A., George, G. N., Pickering, I. J., Prince, R. C., Morel, F. M. M., "Biochemistry: A cadmium enzyme from a marine diatom" *Nature*. **2005**, *435*, 42.
- [14] Tripp, B. C., Smith, K., Ferry, J. G., "Carbonic anhydrase: new insights for an ancient enzyme" *J. Biol. Chem.* **2001**, *276*, 48615-48618.
- [15] Xu, Y., Feng, L., Jeffrey, P. D., Shi, Y., Morel, F. M. M., "Structure and metal exchange in the cadmium carbonic anhydrase of marine diatoms" *Nature* **2008**, *452*, 56-61.
- [16] Cox, E. H., McLendon, G. L., Morel, F. M. M., Lane, T. W., Prince, R. C., Pickering, I. J., George, G. N., "The active site structure of *Thalassiosira weissflogii* carbonic anhydrase 1" *Biochemistry* **2000**, *39*, 12128-12130.
- [17] Brand, U., Vahrenkamp, H., "A new tridentate N,N,S ligand and its zinc complexes" *Inorg. Chem.* **1995**, *34*, 3285-3293.
- [18] Mikuriya, M., Jian, X., Ikemi, S., Kawahashi, T., Tsutsumi, H., Nakasone, A., Lim, J., "Synthesis and characterization of thiolato-bridged cadmium(II) complexes with NNS-chelating thiolic ligands" *Inorg. Chim. Acta* **2001**, *312*, 183-187.

- [19] Mikuriya, M., Jian, X., Ikemi, S., Kawahashi, T., Tsutsumi, H., “Synthesis and structural characterization of thiolato-bridged zinc(II) complexes with NNS-Tridentate thiolic ligands” *Bull. Chem. Soc. Jpn.* **1998**, *71*, 2161-2168.
- [20] Kawahashi, T., Mikuriya, M., Nukada, R., Lim, J., “Synthesis and structural characterization of thiolato-bridged tetranuclear palladium(II) complexes with *N,N,S*-tridentate ligands” *Bull. Chem. Soc. Jpn.* **2001**, *74*, 323-329.
- [21] Mikuriya, M., Kotera, T., Adachi, F., Handa, M., Koikawa, M., Okawa, H., “Syntheses and structural characterization of dinuclear and trinuclear iron(II) complexes of tridentate thiolic ligands with an NNS donor set” *Bull. Chem. Soc. Jpn.* **1995**, *68*, 574-580.
- [22] Mikuriya, M., Adachi, F., Iwasawa, H., Handa, M., Koikawa, M., Okawa, H., “Syntheses and characterization of thiolate-bridged manganese(II) complexes with NNS-tridentate thiolic ligands” *Bull. Chem. Soc. Jpn.* **1994**, *67*, 3263-3270.
- [23] Lai, W., Berry, S. M., Kaplan, W. P., Hain, M. S., Poutsma, J. C., Butcher, R. J., Pike, R. D., Bebout, D. C., “Carbonate templated self assembly of an alkylthiolate bridged cadmium macrocycle” *Inorg. Chem.* **2013**, *52*, 2286-2288.
- [24] Lai, W., Berry, S. M., Tran, A. Q. A., Kaplan, W. P., Glauber, B., Winslow, S. E., Bowman IV, J. I., Poutsma, J. C., Pike, R. D., Bebout, D. C., *Personal Communications* **2013**.
- [25] Gebreyes, K., Shaikh, S. N., Zubieta, J., “Structure of μ -oxo-bis{[*N*-(2-mercaptoethyl)-*N',N'*-dimethylethylenediamino]dioxomolybdenum(VI)}, [Mo₂O₅{(CH₃)₂NCH₂CH₂NHCH₂CH₂S}]₂” *Acta Crystallogr., Sect. C: Cryst. Struct. Commun.* **1985**, *41*, 871-873.
- [26] Shaikh, S. N., Zubieta, J., “Synthesis and structural characterization of a binuclear molybdenum—hydrazido(2-) complex, [Mo₂O₄(NNPh₂){(CH₃)₂NCH₂CH₂NHCH₂CH₂S}]₂” *Inorg. Chim. Acta* **1988**, *144*, 147-148.
- [27] Winslow, S. E., Winer, B. Y., Fukuda, Y., Hain, M. S., Berry, S. M., Pike, R. D., Bebout, D. C., *Personal Communications* **2014**.

- [28] Gasiewicz, T. A., Smith, J. C. "Interactions of cadmium and selenium in rat plasma in vivo and in vitro" *Biochim. Biophys. Acta* **1976**, 428, 113-122.
- [29] Yoneda, S., Suzuki, K. T., "Detoxification of mercury by selenium by binding of equimolar Hg-Se complex to a specific plasma protein" *Toxicol. Appl. Pharmacol.* **1997**, 143, 274-280.
- [30] Yoneda, S., Suzuki, K. T., "Equimolar Hg-Se complex binds to selenoprotein P" *Biochem. Biophys. Res. Commun.* **1997**, 231,7-11.
- [31] Batsanov, S. S., "Van der Waals Radii of Elements" *Inorg. Mater.* **2001**, 37, 1031-1046.
- [32] Thone, C., Vancea, F., Jones, P. G., "Private Communication" *Cambridge Crystallographic Database (v. 5.32 updated Nov 2013)* **2010**.
- [33] Durot, S., Policar, C., Cisnetti, F., Lambert, F., Renault, J., Pelosi, G., Blain, G., Hafsa, K., Mahy, J., "Series of Mn complexes based on *N*-centered ligands and superoxide-reactivity in an anhydrous medium and SOD-like activity in an aqueous medium correlated to MnII/MnIII redox potentials" *Eur. J. Inorg. Chem.* **2005**, 3513–3523.
- [34] Oberhausen, K. J., O'Brien, R. J., Richardson, J. F., Buchanan, R. M., "New tropodal Cu(II) complexes containing imidazole ligands" *Inorg. Chim. Acta* **1990**, 173, 145–154.
- [35] Bebout, D. C., Garland, M. M., Murphy, G. S., Bowers, E. V., Abelt, C. J., Butcher, R. J., "Investigation of the mercury(II) coordination chemistry of tris[(1-methylimidazol-2-yl)methyl]amine by X-ray crystallography and NMR" *Dalton Trans.* **2003**, 2578–2584.
- [36] Roziere, J., Williams, J. M., Stewart, R. P. (Jr), Petersen, J. L., Dahl, L. F., "Cadmium-113 nuclear magnetic resonance studies of ¹¹³Cd(II)-substituted human carbonic anhydrase b" *J. Am. Chem. Soc.* **1977**, 99, 4499-4500.
- [37] Rose, S. L., Hoskin, R. E., Cavanaugh, J. E., Smith, C. J., Blinn, E. L. "The effect of NNS type ligands on the stereochemistry and electronic properties of nickel(II) complexes" *Inorg. Chim. Acta* **1980**, 40, 7-13.

- [38] Marabella, C. P., Enemark, J. H., Miller, K. F., Bruce, A. E., Pariyadath, N., Corbin, J. L., Stiefel, E. I. "Complexes containing the $\text{Mo}_2\text{O}_5^{2+}$ core: preparation, properties, and crystal Structure of $\text{Mo}_2\text{O}_5[(\text{CH}_3)_2\text{NCH}_2\text{CH}_2\text{NHCH}_2\text{C}(\text{CH}_3)_2\text{S}]_2$ " *Inorg. Chem.* **1983**, 22, 3456–3461.
- [39] Bhasin, K. K., Singh, J., and Singh, K. N., "Preparation and characterization of 2,2'-dipicolyl diselenide and their derivatives" *Phosphorus, Sulfur and Silicon* **2002**, 177, 597-603.
- [40] Torubaev, Y. V., Pasynskii, A. A., Pavlova, A. V., "Diphenyldichalcogenide complexes of iron, chromium and rhenium carbonyls" *Koord.Khim.(Russ.)(Coord.Chem.)* **2012**, 38, 724-732.
- [41] Sau, Y., Yi, X., Chan, K., Lai, C., Williams, I. D., Leung, W., "Insertion of nitrene and chalcogenolate groups into the Ir-C σ bond in a cyclometalated iridium(III) complex" *J. Organomet. Chem.* **2010**, 695, 1399-1404.
- [42] Bates, C. M., Morley, C. P., Di Vaira, M., "Pentamethylcyclopentadienylselenium derivatives: synthesis and x-ray crystal structures of $[\text{M}(\text{CO})_5\{\text{Se}2(\sigma\text{-C}_5\text{Me}_5)_2\}]$ ($\text{M} = \text{Cr}, \text{W}$)" *Chem. Commun.* **1994**, 2621-2622.
- [43] Kienitz, C. O., Thöne, C., Jones, P. G., "Coordination Chemistry of 2,2'-Dipyridyl Diselenide: X-ray Crystal Structures of PySeSePy , $[\text{Zn}(\text{PySeSePy})\text{Cl}_2]$, $[(\text{PySeSePy})\text{Hg}(\text{C}_6\text{F}_5)_2]$, $[\text{Mo}(\text{SePy})_2(\text{CO})_3]$, $[\text{W}(\text{SePy})_2(\text{CO})_3]$, and $[\text{Fe}(\text{SePy})_2(\text{CO})_2]$ ($\text{PySeSePy} = \text{C}_5\text{H}_4\text{NSeSeC}_5\text{H}_4\text{N}$; $\text{SePy} = [\text{C}_5\text{H}_4\text{N}(2\text{-Se})\text{-N,Se}]$) *Inorg. Chem.* **1996**, 35, 3990-3997.
- [44] Eriksson, A.E., Jones, T.A., Liljas, A., "Refined structure of human carbonic anhydrase II at 2.0 Å resolution" *Proteins* **1988**, 4, 274-282.